ANTENNA LABORATORY

Technical Report No. 2

BROADBAND ARRAYS OF HELICAL DIPOLES

by
D. T. STEPHENSON
P. E. MAYES

Contract No. NEL 30508A

January 1964

Part 2 of Final Report
Covering the Period June 1, 1962 - August 31, 1963

Sponsored by
U.S. NAVY ELECTRONICS LABORATORY
San Diego, California

DEPARTMENT OF ELECTRICAL ENGINEERING
ENGINEERING EXPERIMENT STATION
UNIVERSITY OF ILLINOIS
URBANA, ILLINOIS

Antenna Laboratory

Technical Report No. 2

BROADBAND ARRAYS OF HELICAL DIPOLES

by

D. T. Stephenson
P. E. Mayes

Contract No. NEL 30508A

January 1964

Part 2 of Final Report
Covering the Period June 1, 1962 - August 31, 1963

Sponsored by

U.S. NAVY ELECTRONICS LABORATORY
San Diego, California

Department of Electrical Engineering
Engineering Experiment Station
University of Illinois
Urbana, Illinois

CONTENTS

ILLUSTRATIONS

ACKNOWLEDGEMENT

The authors acknowledge with thanks the work of Henry Hegener, Werner Lain, Sam Kuo, and Edward McBride, student technicians in the Antenna Laboratory.

1. INTRODUCTION

Research on frequency-independent antennas took a giant step forward with the introduction of the "angle concept" by Rumsey[1] in 1954. This principle states that a radiating structure can feature patterns and input impedances that are independent of frequency, provided that its geometry is such that it can be described in terms of angles instead of linear dimensions. In the years that followed, this principle was applied in many different ways to produce antennas of widely varying configurations.

Common to all such designs, however, is a basic limitation on size: if the antenna is to operate at any given frequency, some dimension of the structure is of the order of one-half of a free-space wavelength at that frequency. Therefore a broadband antenna, the low-frequency limit of which is, say, three megacycles, has to be quite large. This size requirement may not be a serious problem in a fixed, ground-based installation where a lot of land is available. On shipboard, however, the problem becomes important. Practical frequency-independent designs are, to some extent, directional in their radiation characteristics; therefore it is desirable to mount a shipboard antenna so that it can be rotated. A low-frequency antenna would thus require a large, unobstructed circular area if it were mounted near the deck of the ship. If it were mounted on top of a mast, its weight, rigidity, and support would become a problem. A need exists, therefore, for a size-reduced frequency-independent antenna array.

The first problem is to determine which type of frequency-independent design best lends itself to some means of size reduction. One class of such antennas features a geometry which is repeated periodically with the logarithm of distance from the apex of the structure; these are called "log-periodic" structures. Isbell,[2] in 1959, replaced the sheet-metal teeth on one of these log-periodic structures with conventional half-wave dipoles; thus the log-periodic dipole array was created. Now a very popular antenna, it was the first application of the log-periodic principle to an array of conventional radiating elements. Several ways of reducing the resonant length of a dipole are known, and have been used for many years. Therefore it was decided that the log-periodic dipole (LPD) array would be the starting point for the size-reduction program.

The most complete analysis and design procedure to date for an LPD is by Carrel.[3] His paper outlines the history of LPD development, gives a thorough description of its construction and operation, analyzes the antenna mathematically,

and provides a complete set of design charts for those who want to build their own. It has been the basis of all of the work discussed in this chapter, and it will be referred to in suceeding sections.

Figure 1.1 is a photograph of of an LPD array, built for testing in the Antenna Laboratory. The coaxial cable, through which the antenna is fed, travels through one of the feeder tubes to the small end of the antenna; it is at this point that the antenna is actually fed. Here the wave is applied to the feeder, the twin-wire transmission line which runs to the shorting block behind the longest dipole. The wave travels down the feeder, away from the feedpoint, past those dipoles which are too short to be resonant at the applied frequency. The section of the antenna which contains these dipoles is called the "transmission region". Beyond the transmission region is the "active region", the region containing those dipoles which are resonant at frequencies in the neighborhood of the applied frequency. In the active region, the energy in the feeder wave is radiated by the dipoles. If the active region efficiency is high, there is practically no energy left on the feeder beyond the active region, and the remainder of the antenna, containing dipoles longer than resonant length, is called the "unexcited region". It is the presence of this unexcited region which allows the antenna to be terminated at any desired length without affecting its properties as seen from the feedpoint.

Proper operation of an LPD depends on the dipole currents in the active region being phased in such a way as to produce radiation back over the feedpoint, off the small end of the antenna. A periodic radiating structure, in which radiation occurs in the direction opposite to that of the exciting (feeder) wave, is said to be a "backfire" radiator. Therefore the term "backfire" is used to describe the proper mode of operation of an LPD, even though the radiation is actually "endfire" in terms of what is usually defined as the "front end" of the antenna, i.e., the end containing the feedpoint.

In addition to the dipole-length problem for an LPD at low frequencies, there is a requirement on boom length (feeder length): directivity suffers if the antenna is made too short for a given operating bandwidth. Although an array that is size-reduced in one direction only may be quite useful, overall size reduction would require reduction in both dipole lengths and boom length. For this reason, while primary emphasis is given in this report to dipole shortening, the boom-length problem is brought in wherever it is applicable. It is worth noting that the

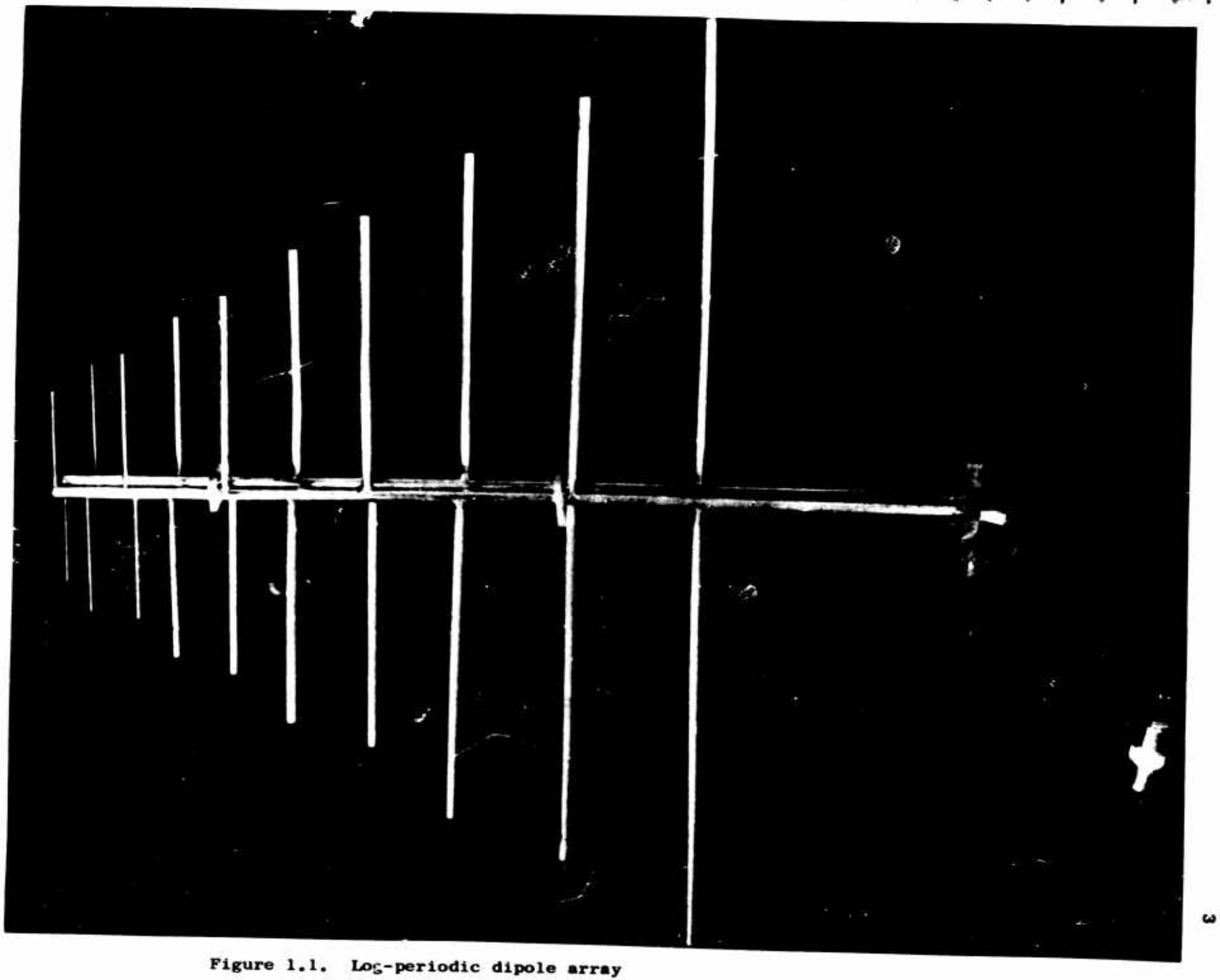

Figure 1.1. Log-periodic dipole array

radiation pattern of a short dipole is nearly the same as that of a half-wavelength dipole, therefore dipole length alone should have very little effect on directivity.

Succeeding sections of this chapter describe the work done on size reduction of LPD arrays. Section 1.1 discusses the method used for dipole shortening, and describes the models used for laboratory testing. Section 1.2 presents the results of this testing, including efforts towards optimization of the performance of size-reduced arrays. Section 1.3 describes a type of antenna which combines a conventional LPD with a size-reduced LPD. Data on its performance are presented, together with a discussion of possible ways of improving it. All experimental results are summarized in Section 1.4 and the capabilities and usefulness of size-reduced arrays are discussed. Included in the References is a brief review of each of the references cited in this chapter.

1.1 Dipole Length Reduction and the Log-Periodic Helical Dipole Array

The method chosen for shortening the dipoles in the LPD array is to replace them with normal-mode helical dipoles. By the proper choice of pitch angle and other helix parameters, a helical dipole may be made to resonate at a frequency much lower than the frequency for which the dipole is a half-wavelength long.

This method was chosen in preference to inductive base-loading because of its higher efficiency, and in preference to capacitive end-loading because of the fact that such end-loading would require a lot of weight hanging out on the ends of each dipole. Dielectric-loading of the entire array is impractical at low frequencies. The helical dipole also features a uniform geometry which simplifies the construction.

In the following paragraphs are found a brief discussion of helical dipoles and their characteristics, and a description of the logarithmically-periodic helical dipole array (LPHDA).

1.1.1 Normal-Mode Helical Dipoles

The normal-mode helical dipole differs from the more common axial-mode or helical beam antenna in that its diameter is on the order of one-tenth wavelength or less at the frequency of operation. Its radiation pattern is similar to that of a linear half-wave dipole. Detailed analyses have been made by such authors as Wheeler,[4] Kraus,[5] Kandoian and Sichak,[6] and Li.[7]

In Figure 1.2 are sketched two dipoles, one a half-wave linear dipole, the other a helical dipole. The degree of shortening of the helical dipole compared

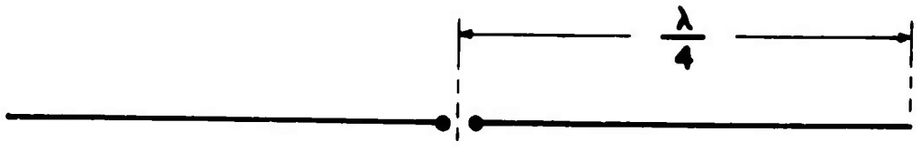

LINEAR HALF-WAVE DIPOLE

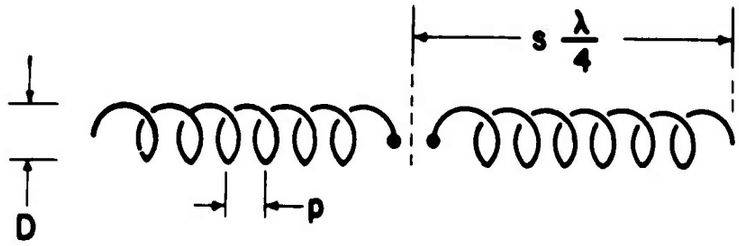

HELICAL HALF-WAVE DIPOLE

Figure 1.2. Linear and helical dipoles

to the linear one is denoted by the factor s, $0 \leq s \leq 1$. As a very rough first approximation, it may be assumed that a wave travels down the helix with the velocity of light, but in the direction of the helical path described by the wire. Thus the phase velocity in the direction of the helix axis is lower than that of free space, and is related to the ratio of pitch p to diameter D. Accordingly, the "guide wavelength" λg, i.e., the wavelength in the axial direction, is less than the free-space wavelength, λ. The resonant length of the helical dipole would then be one-half of a guide wavelength, but less than half of a free-space wavelength. resonant length = $\lambda g/2 = s\,\lambda/2$.

In order to make any use of helical dipoles, one must know which dipole dimensions will result in a specified resonant frequency and a specified shortening factor s. The approximation used above, which says essentially that the total length of wire in the dipole should be $\frac{\lambda}{2}$ when unwound, is not satisfactory except as a starting point for a cut-and-try method of dipole design. Existing design data[6,7] do not take into account wire size, for example, but wire size was found (in measurements on helical dipoles and monopoles) to have a major effect on resonant frequency. In order to provide some more useful design data, a number of measurements were performed on helical dipoles. The results of these measurements are discussed in Appendix A.

There are several reasons why the use of helical dipoles in place of linear dipoles would be expected to change the performance of the array. The radiation resistance of a helical dipole drops as s is reduced below unity. In a log-periodic array the active region efficiency is somewhat dependent on the relationship between dipole impedance and feeder impedance, therefore it would be expected that the substitution of helical dipoles would change the active region efficiency, and therefore directivity, end effect, etc. Mutual impedances between dipoles in the array would also be expected to differ from those in an array of linear dipoles. mutual impedances have a similar effect on LPD performance.

Unlike a linear dipole, the helical dipole produces elliptically-polarized radiation, but in the range of dipole parameters used in this investigation this effect was found to be quite small and the polarization nearly linear.

Underlying the entire idea of antenna size reduction are certain basic rules which make it impossible to combine in one antenna high efficiency and gain with

small size in wavelengths.[8,9]

These considerations lead one to expect a certain degree of deterioration in the performance of the LPHDA as dipole lengths are reduced. A major purpose of this investigation has been to determine to what degree one must compromise in return for obtaining a narrower array.

1.1.2 The Log-Periodic Helical Dipole Array

Except for the dipoles themselves, the LPHDA is very similar to the conventional LPD array. The effective 180-degree twist in the feeder from one dipole to the next, the construction of the feed point, the use of a coaxial cable through one side of the feeder to drive the antenna, etc., are all in accordance with conventional LPD design.

Figure 1.3a illustrates the parameters used to describe the array. These correspond to the parameters used in LPD design, except that the spacing factor σ is now defined in terms of the free-space wavelength, λ_n, at the resonant frequency of the n^{th} dipole, instead of the length of the n^{th} dipole. Figure 1.3b shows the way in which the dipoles are connected to the feeder.

The method of construction of laboratory models was dictated by measurement requirements. These are discussed in Appendix B. The feed cables for the LPHDA models (and the LPD models built for comparison purposes) were made from RG-141 cable, a teflon-dielectric type similar in size to RG-58. Silver tubing, just large enough to contain RG-141 cable with its outer fiberglass cover removed, was used for the feeders. The dipoles themselves were wound with copper or tinned copper wire on cylindrical polystyrene rods. The wire was soldered to the feeder, usually with conventional tin-lead solder, and the polystyrene rods were glued to the feeder for mechanical support (except for the variable - σ models). All helix dimensions were scaled by the factor τ as closely as standard A.W.G. wire sizes permitted. A shorting plate was soldered across the rear end of the feeder, at a distance $\lambda/8$ behind the longest dipole. A cut-and-try technique was used to design the dipoles themselves to make them resonant at the desired frequencies.

In Section 1.4 of this chapter some comments are made on the construction of LPHDA antennas for operation in and above the HF (3 to 30 Mc) range.

1.2 Experimental Investigations and Results

Extensive experimental work on LPD antennas, performed in the Antenna Laboratory, has produced a wealth of data with which LPHDA models could be compared. For this reason, the LPHDA experimental investigations have been based on previous (and

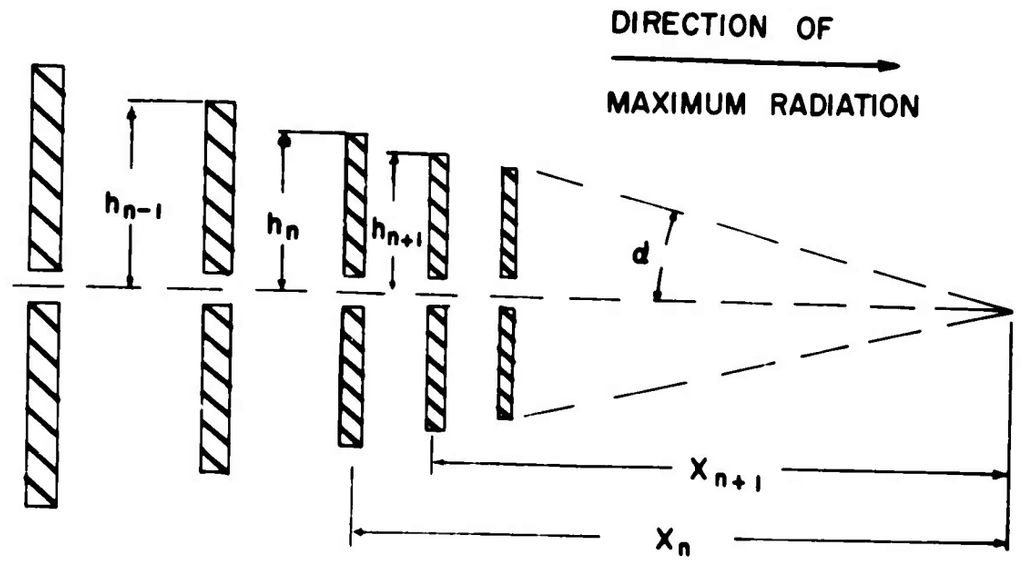

$$\frac{X_{n+1}}{X_n} = \frac{h_{n+1}}{h_n} = \tau \qquad \frac{X_n - X_{n+1}}{\lambda_n} = \sigma \qquad h_n = s\frac{\lambda_n}{4}$$

Figure 1.3a. Parameters of an LPHDA.

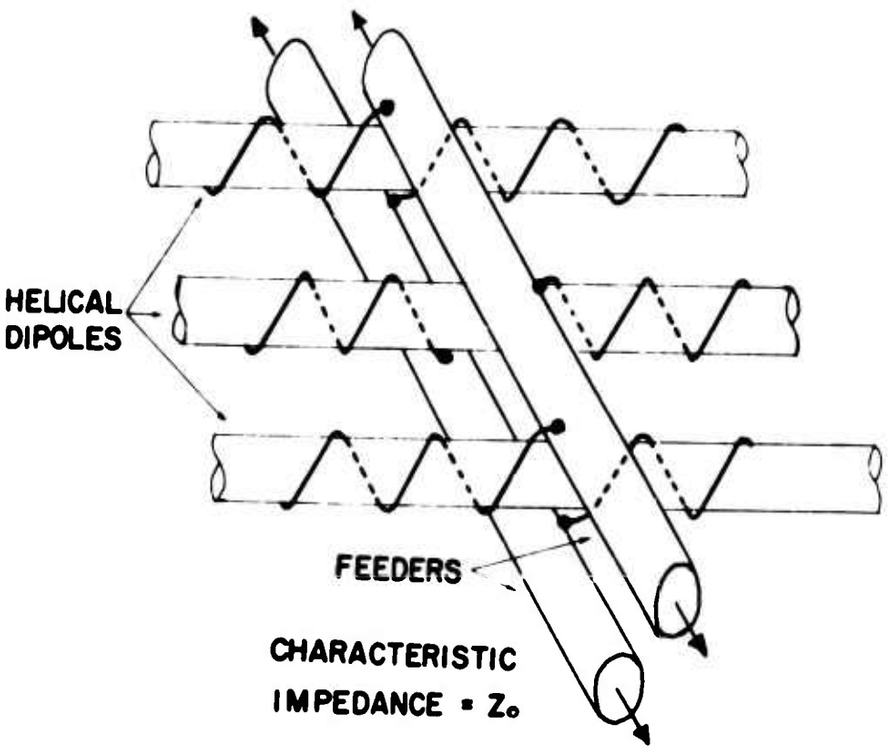

Figure 1.3b. Feeder and dipole detail of an LPHDA.

current) LPD measurements. A description of the techniques used, together with block diagrams of the test equipment connections, is found in Appendix B.

Wherever directivity is mentioned in this report, it was calculated from the approximate formula:[5]

$$\text{Directivity in decibels} = 10 \log \frac{41{,}263}{(BW)_E \, (BW)_H}$$

where $(BW)_E$ and $(BW)_H$ are the half-power beamwidths, in degrees, in the E-plane and the H-plane, respectively. Whenever values of VSWR are mentioned, these are maximum values of VSWR with respect to the mean value of input impedance over the entire given frequency range (although individual impedance points that are isolated from the remainder of the points on the Smith Chart are occasionally discarded from the VSWR calculation).

1.2.1 Active Region Efficiency vs. s

It is clear that a very small degree of dipole shortening (s close to 1) would result in an array the performance of which is nearly the same as that of an ordinary LPD. But such an array would be of no value where size reduction is an important factor. The first problem, then, was to determine a range of values of s in which both satisfactory performance and appreciable size reductions could be obtained.

Two pattern models were built, each uniformly periodic; that is, the scale factor τ was unity, all dipoles resonated at the same frequency, and the dipoles were spaced uniformly along the feeder. Such an antenna is not a broadband device, but it is useful in predicting the performance of broadband, log-periodic arrays in certain respects; Section 1.2.4 discusses its properties in greater detail.

Each of the uniformly-periodic models contained five dipoles. The same dipole spacing was used on each, and their feeders were of equal length and open-circuited at the ends opposite the feedpoints. Their feeder characteristic impedances, Z_o, could be varied. The difference between these models was that the shortening factor s was equal to 0.26 on the first model, and 0.57 on the second.

Figure 1.4 shows, in solid lines, the far-field radiation patterns of these two antennas. While the second model (s = 0.57) exhibited undirectional backfire radiation at the dipole resonant frequency, the first model (s = 0.26) featured a strongly bidirectional pattern. Only when five more dipoles were added to the

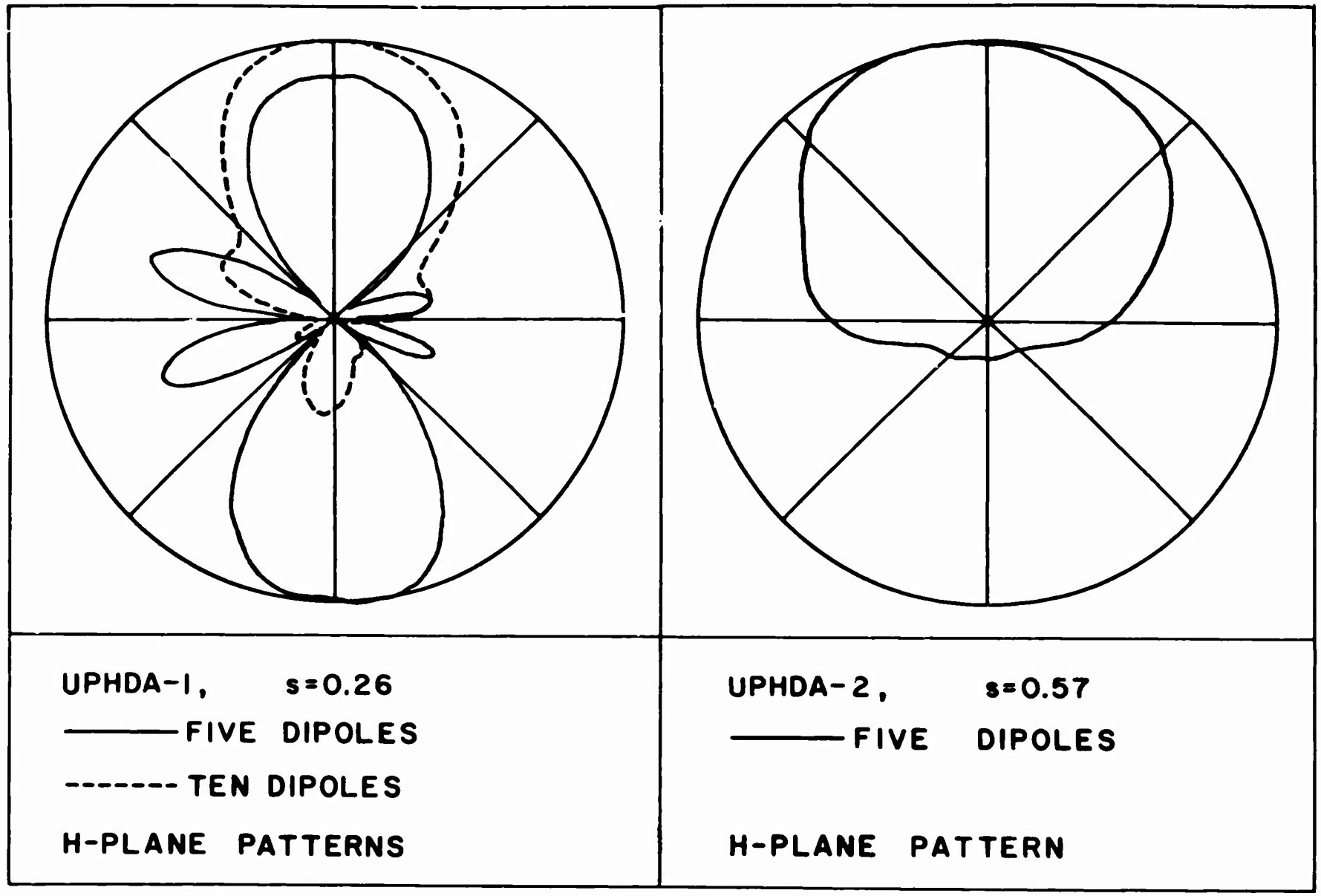

Figure 1.4 Radiation patterns of UPHDA - 1 and 2

first array, giving it a total of ten dipoles, did it exhibit backfire radiation (broken line in Figure 14). Further pattern measurements, taken at different values of Z_o, all showed the same effect.

These results illustrate a strong dependence of the efficiency of the active region upon the value of s. In the s = 0.26 model, each of the original five dipoles radiated relatively little of the energy that was propagated towards them along the feeder. The remainder of the energy continued to the rear end of the feeder, and was reflected back towards the feed point. This reflected signal excited the dipoles once again, producing strong radiation in a direction opposite to that produced by the incident feeder signal; hence the bidirectional pattern. A log-periodic array built with such a low value of s would therefore suffer from strong end-effect and poor front-to-back ratio, unless the scale factor τ were very close to unity. Such a τ would lead to an extremely long antenna for any appreciable operating bandwidth.

For this reason, it was decided that a value of s in the range 0.5 to 0.6 would be used in subsequent size-reduced models. This should be kept in mind as experimental results in the following sections are studied; the levels of performance obtained with such LPHDA models could not necessarily be expected to hold for lower values of s. Further work would be necessary in order to determine favorable design parameters for arrays with smaller s.

1.2.2 Direct Comparison of Arrays of Linear and Helical Dipoles

To gain further insight into the effect of dipole shortening, two pairs of log-periodic arrays were built. In each pair, the models were identical except that one was built with linear dipoles while the other had helical dipoles. The first pair, LPD-1 and LPHDA-1, was based on Carrel's "optimum" design for 9.5 db directivity; the second pair, LPD-2 and LPHDA-2, was based on minimum boom length for 9 db directivity.[3] It was discovered, after construction and testing of the first pair, that the helical dipole design had been in error and that the frequency range of LPHDA-1 was different from that of LPD-1; therefore a direct comparison could not be made. The dipoles in LPHDA-2, however, were designed more carefully. It was on this second pair of antennas that the data presented here were measured. The shortening factor for LPHDA-2 was 0.54.

Figure 15 shows the far-field H-plane radiation patterns of this pair of antennas at four different frequencies. The patterns of LPD-2, represented by dashed lines, are quite consistent over the entire frequency range for which the antenna

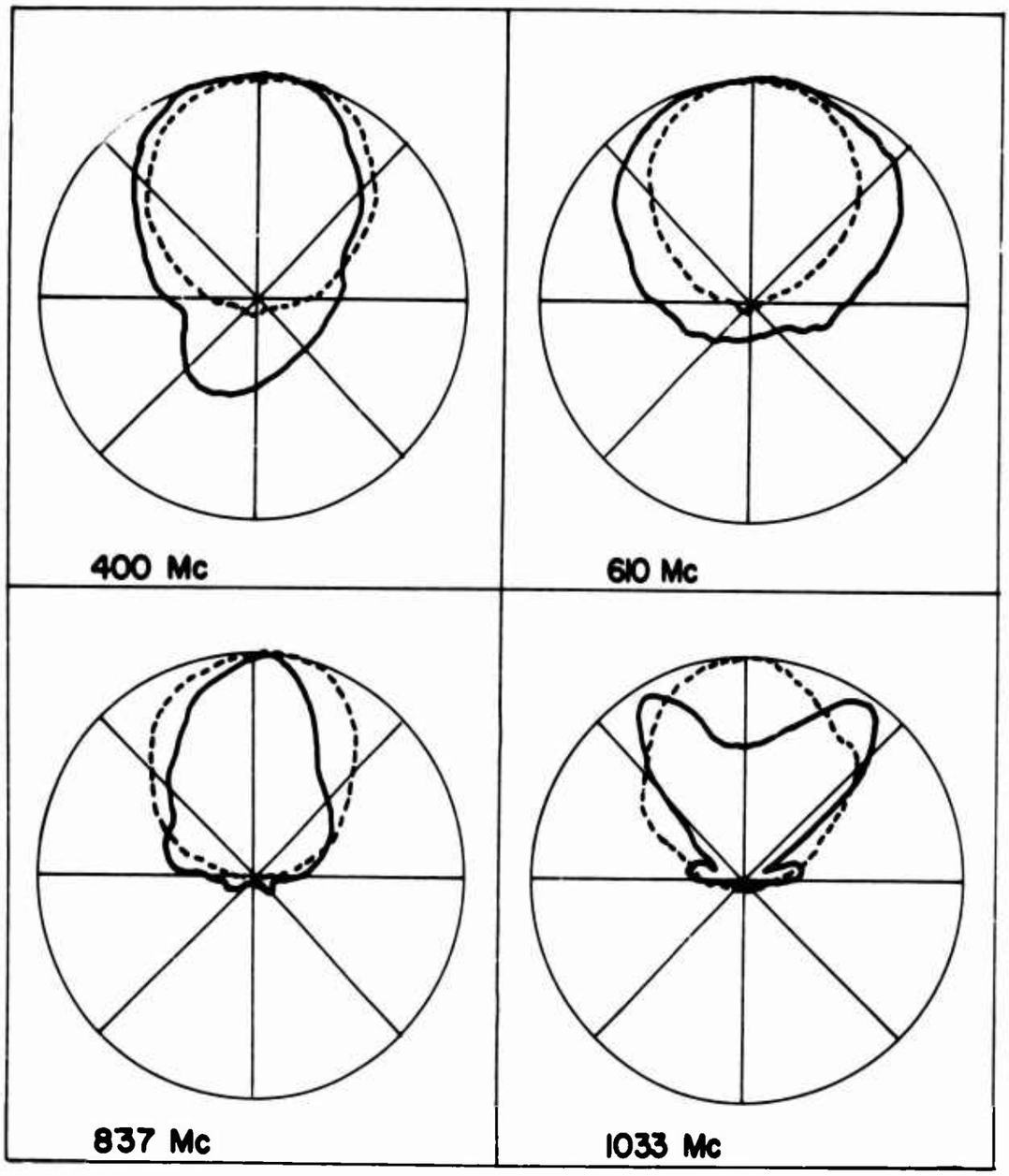

Figure 1.5. Radiation patterns of LPD - 2 and LPHDA - 2

was built (400 to 1000 Mc). By contrast, the patterns of LPHDA-2 (solid lines) deteriorate quite noticeably at the ends of the frequency range (the 400 and 1033 megacycle patterns). This result, like the result discussed in Section 1.2.1, shows that the active region on the LPHDA includes a larger number of dipoles than does the active region on the corresponding LPD.

The 610 Mc pattern is typical of the mid-range performance of the LPHDA. It is seen that both directivity and front-to-back ratio suffer somewhat by comparison with the LPD.

Figure 1.6 illustrates the variation with frequency of the input impedances of the antennas at their feed-points. Impedance readings were taken at three frequencies per log-period; that is, f_n, $\tau^{-1/3} f_n$, $\tau^{-2/3} f_n$, $\tau^{-1} f_n = f_{n+1}$, etc., where f_n is the resonant frequency of the n^{th} dipole. The impedance shown by the individual dots on the Smith Chart are those of the LPHDA, from 400 to 1000 Mc. The circle on the chart encloses <u>all</u> of the LPD impedances over the same frequency range. The VSWR with respect to mean input impedance varies as follows:

LPD:	VSWR = 1.5, 400-1000 Mc.
LPHDA:	VSWR = 4.85, 400-1000 Mc.
	VSWR = 3.2, 400-753 Mc.

Figure 6 does not show the direction of movement of the impedance on the chart as frequency is changed. It is remarked here that the impedance displayed the orderly, clockwise progression, with increasing frequency, that is characteristic of log-periodic arrays.

All of the data obtained on this pair of antennas may be summarized as follows: the LPHDA, built with the same design parameters as the LPD but with s equal to 0.54, featured an operating bandwidth about 65% as wide as that of the LPD, an average directivity of about 6.4 db compared to 9 db for the LPD, an <u>average</u> front-to-back ratio of 15.4 db compared to a <u>minimum</u> of 20 db for the LPD, and the comparison of VSWR given above.

This degradation in performance, of course, was anticipated from the discussion in Section 1.1.1. But there is no reason to assume that optimum performance in an LPHDA should result from the same design parameters as those which lead to optimum performance in an LPD. The next step, therefore, was to determine the degree to which LPHDA performance could be improved by changing the values of various design parameters.

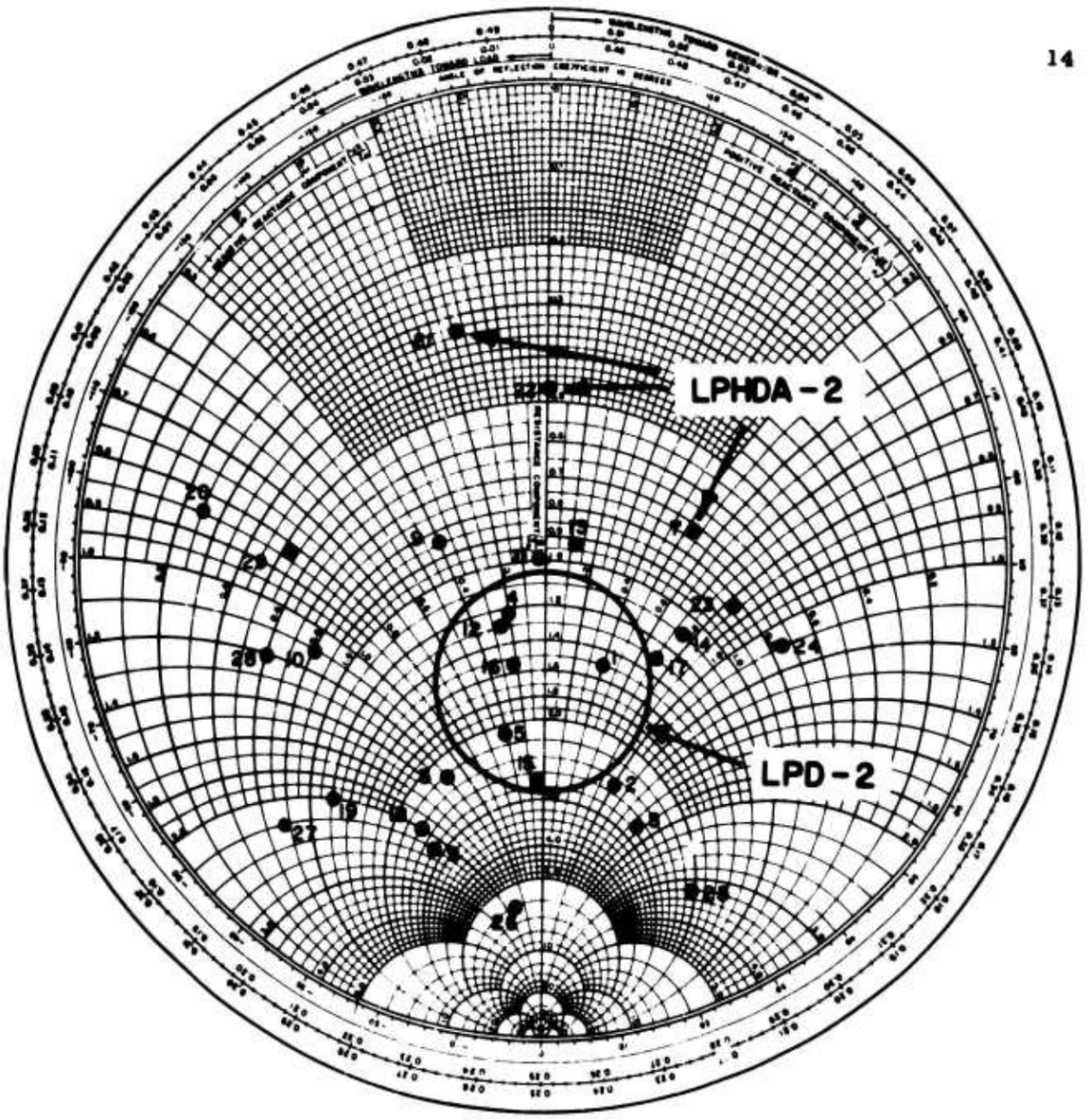

LPD-2 and LPHDA-2 (s = 0.54)

σ = 0.10 τ = 0.90 400 - 1000 Mc

Point	Freq.	Point	Freq.	Point	Freq.
1	400 Mc.	11	568 Mc.	21	809 Mc.
2	414	12	589	22	837
3	429	13	610	23	866
4	444	14	631	24	897
5	460	15	655	25	929
6	477	16	678	26	962
7	494	17	702	27	998
8	511	18	727	28	1033
9	530	19	753	29	1069
10	549	20	779		

Figure 1.6. Input impedance of LPD-2 and LPHDA -2

1.2.3 LPHDA Performance vs. τ, σ, and Z_o

The goal in this investigation was to determine which values of τ, σ, and Z_o lead to optimum performance of an LPHDA with $s \tilde{=} 0.5$, in terms of directivity, VSWR, and boom length.

LPHDA models 3, 4, and 5 were built to cover a 400-800 Mc frequency range. These models featured a feeder impedance Z_o of 100 ohms, a shortening factor s of 0.54, and scale factor τ of 0.90, 0.92, and 0.95, respectively. Two of these arrays are shown in Figures 1.7 and 1.8. The dipole core rods were not glued to the feeders, by unsoldering the wires from the feeder one could move the dipoles to any desired location on the feeder. The shortening plate behind the longest dipole could be unsoldered and moved. Small plastic clamps held the feeder to its proper spacing. Measurements of input impedance and far-field patterns, as functions of frequency, were made for several different values of σ on each model.

In Figure 1.9 are shown the results of these measurements, plotted in terms of VSWR. It will be noticed that each of the three antennas featured a value of σ that was "optimum", i.e., that produced the lowest VSWR. Design "A" in Figure 1.9, with τ = 0.90 and σ = 0.16, gave the lowest VSWR, just under 2. But since boom length is directly proportional to σ, design "A" resulted in quite a long antenna. Design "B", the τ = 0.92 model with σ = 0.07, performed almost as well in terms of VSWR (2.2), and was much shorter and more compact. Design "C" with τ = 0.95 and σ = 0.05 featured a VSWR of about 2.5, but it appears to be the most compact array. In reality, however, it is longer than design "B", because the increase in τ more than offsets the decrease in σ. Thus from the standpoint of VSWR and boom length, the best design of these three appears to be design "B". Figure 1.10 shows the impedance pattern for design "B", and Figure 1.11 shows, for comparison, the considerably poorer pattern for the τ = 0.90 array at σ = 0.07.

Figure 1.12 shows the radiation patterns of the design "B" model. Directivity is about 6.5 db, and front-to-back ratio averages 15 db from 400 to 800 Mc and 19 db from 514 to 800 Mc. There were only minor variations in the radiation patterns of the three variable - σ models as σ was changed, but in general the best patterns and the best VSWR were found at approximately the same σ values. For all models, the front-to-back ratio was rather poor over the lowest log-period of frequency; this effect was mentioned earlier in connection with LPHDA-2. At the high-frequency

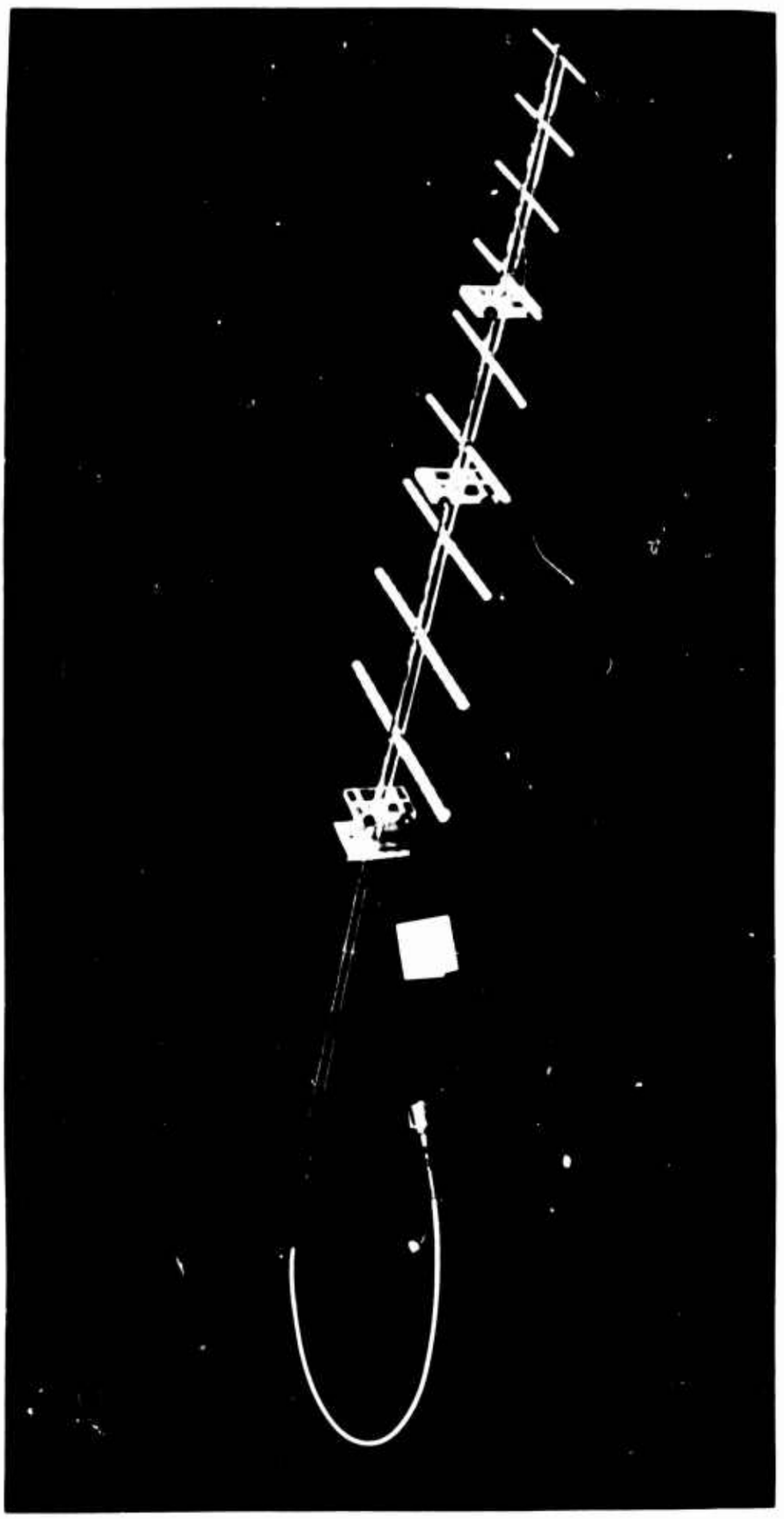

Figure 1.7. Laboratory model LPHDA - 3

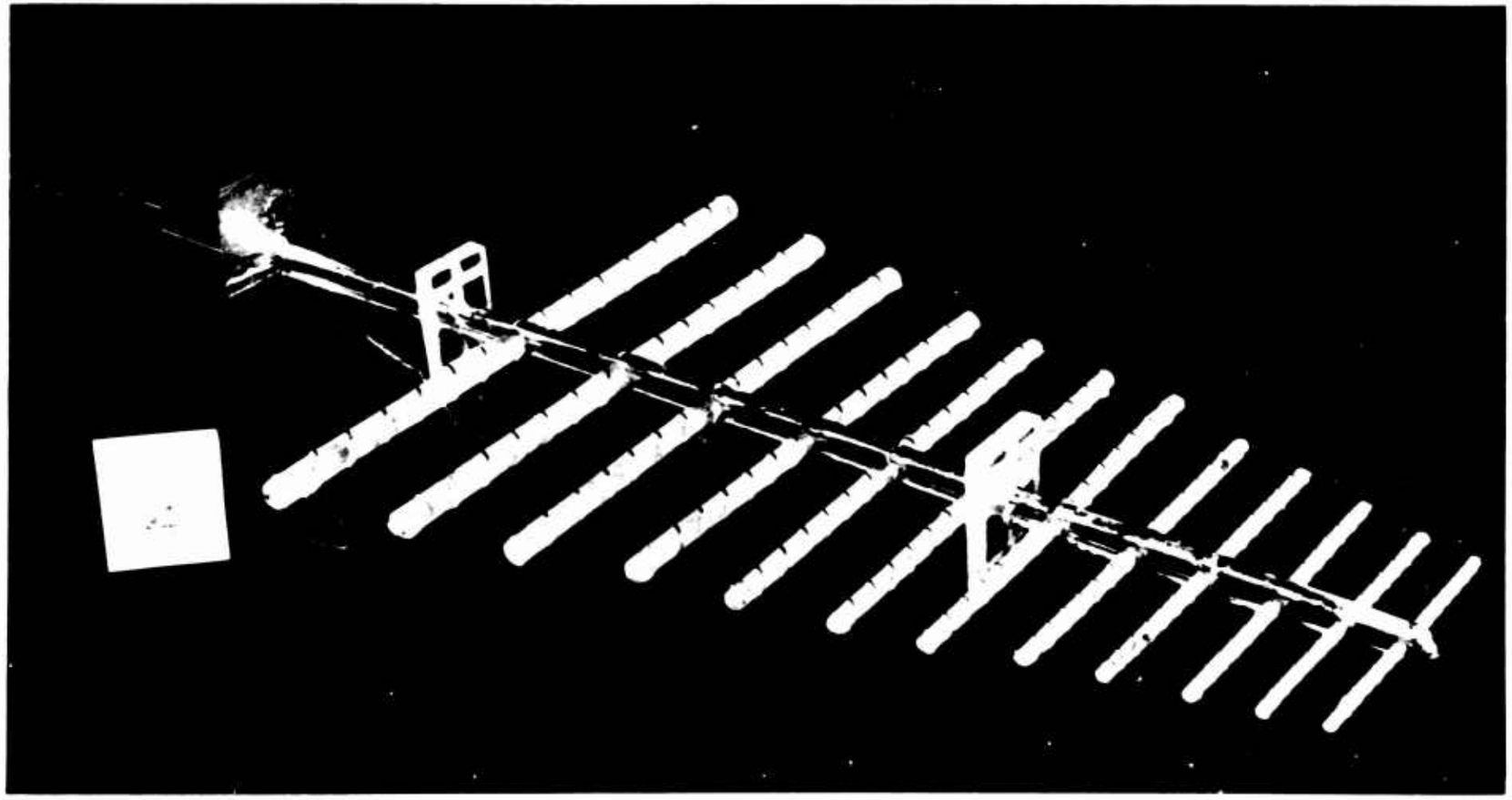

Figure 1.8. Laboratory model LPHDA - 4

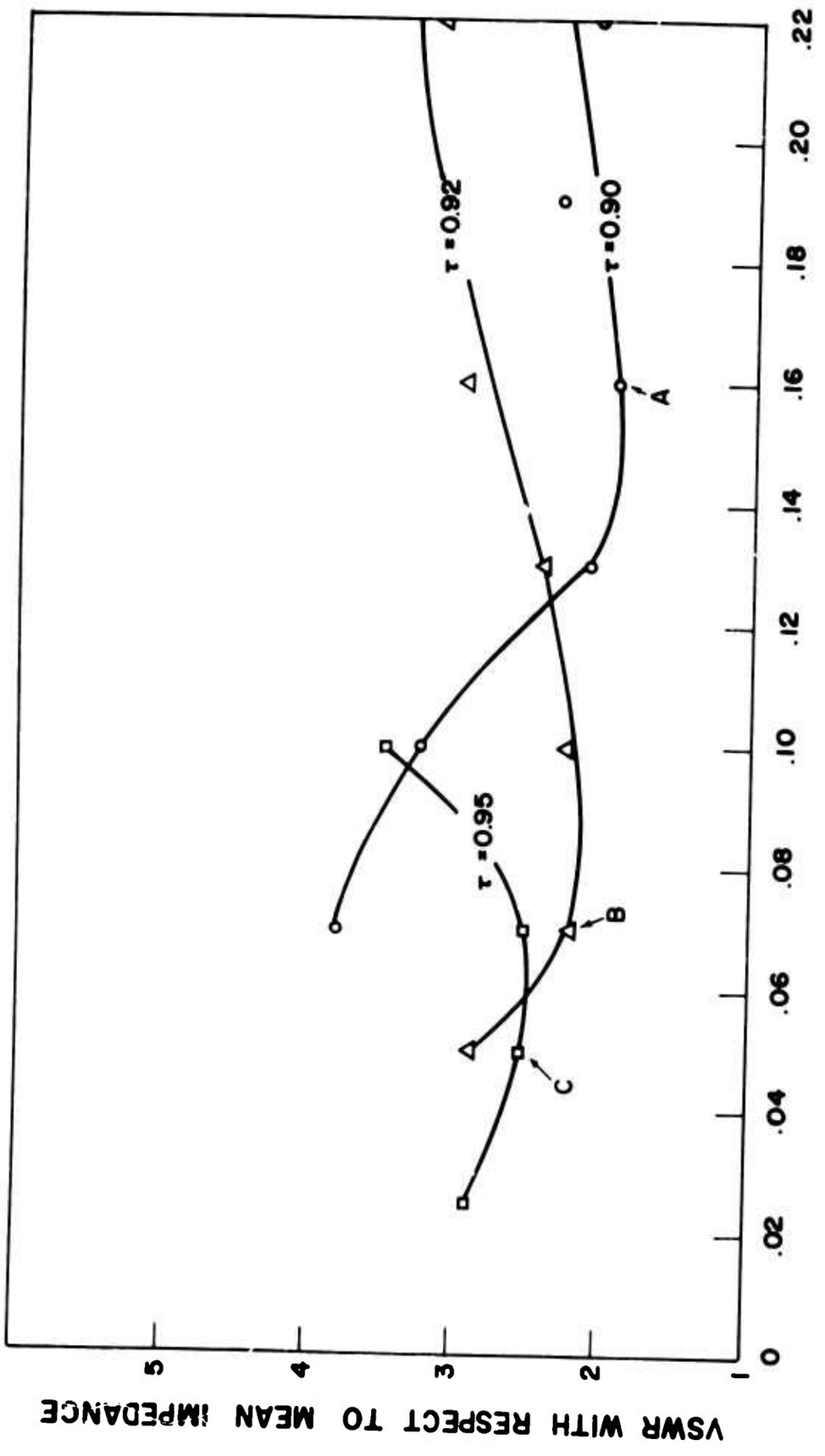

Figure 1.9. VSWR vs. τ and σ; s = 0.54

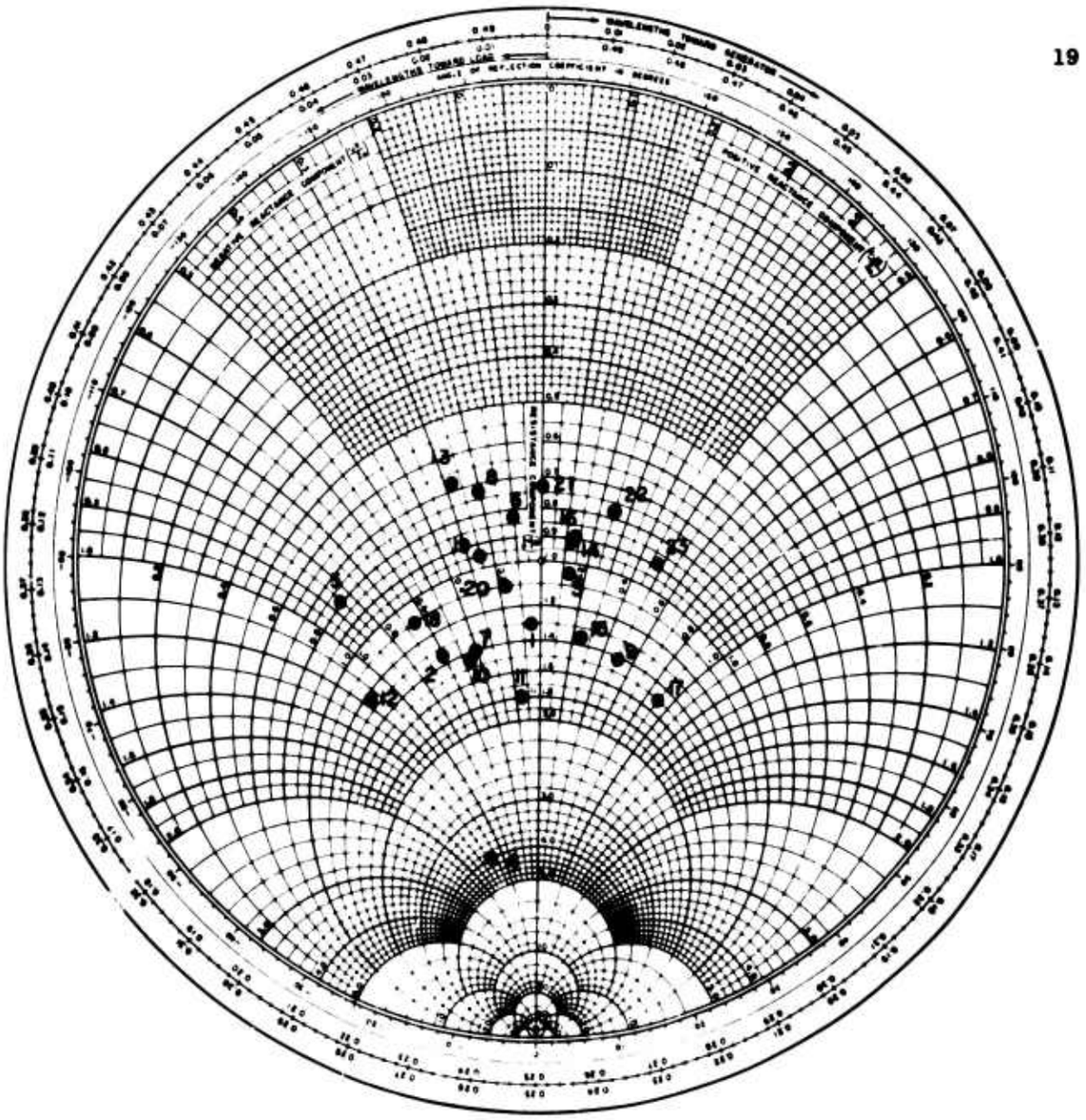

LPHDA - 4 a (S = 0.54)

σ = 0.07 τ = 0.92 414 - 800 Mc

Point	Freq.	Point	Freq.
1	414 Mc.	13	631 Mc.
2	429	14	655
3	444	15	678
4	460	16	702
5	477	17	727
6	494	18	753
7	511	19	779
8	530	20	809
9	549	21	837
10	568	22	866
11	589	23	897
12	610		

Figure 1.10. Input impedance of LPHDA design "B".

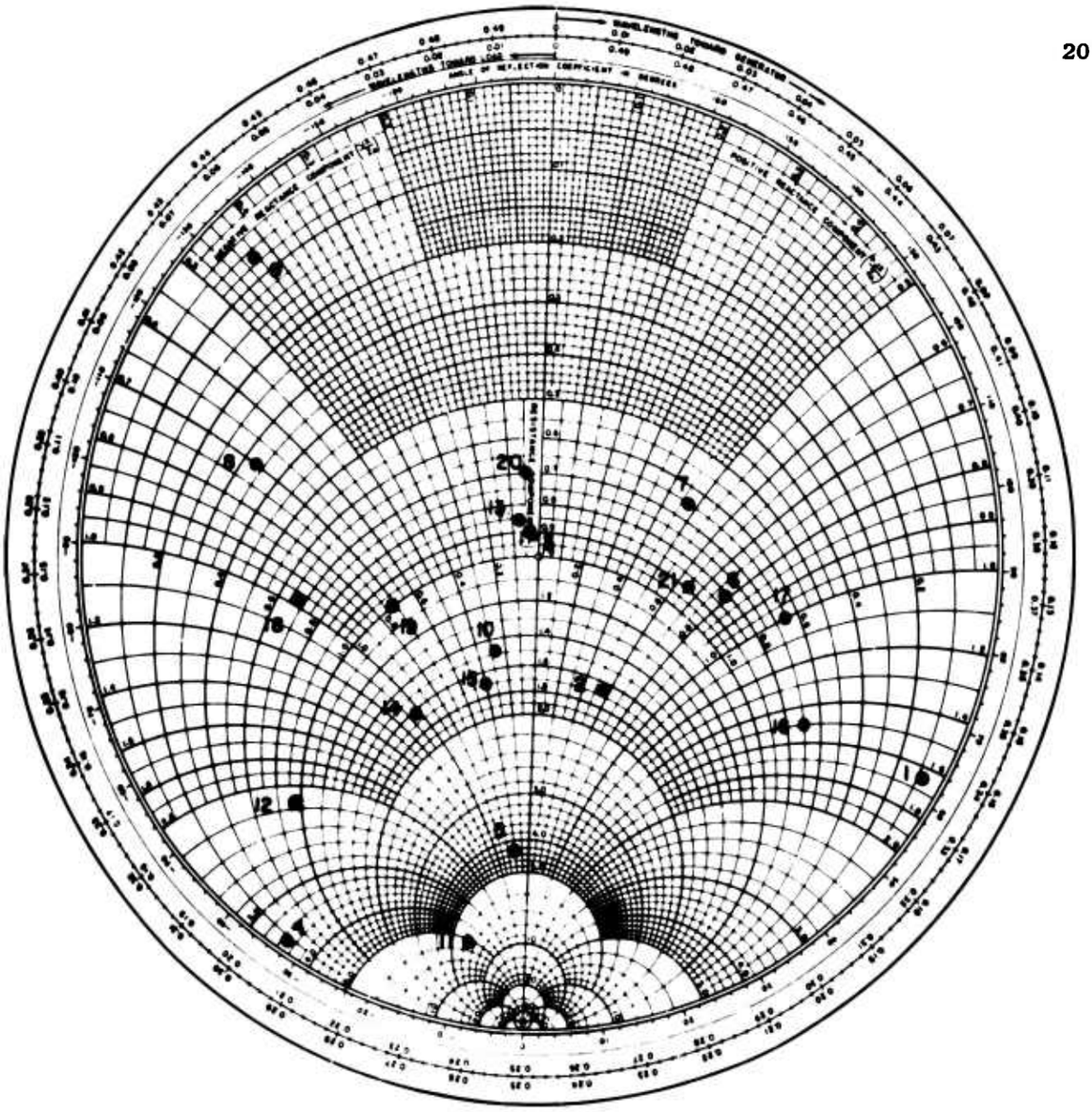

LPHDA-3a (s=0.54)

σ=0.07 τ=0.90 414-800 Mc

Point	Freq.	Point	Freq.
1	400 Mc.	12	589
2	414	13	610
3	429	14	631
4	444	15	655
5	460	16	678
6	477	17	702
7	494	18	727
8	511	19	753
9	530	20	779
10	549	21	866
11	568		

Figure 1.11. Input impedance of poor LPHDA design

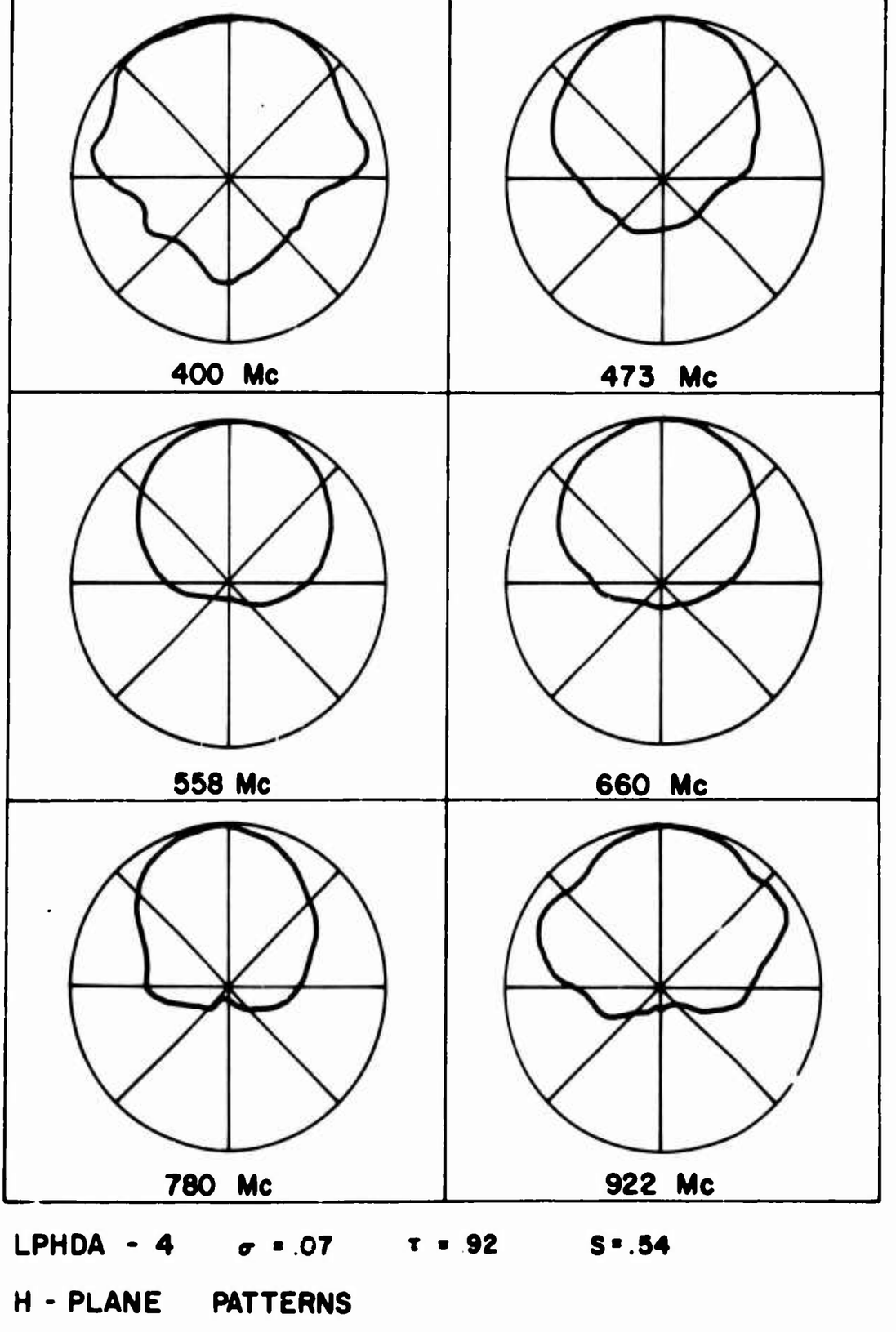

LPHDA - 4 σ = .07 τ = 92 S = .54

H - PLANE PATTERNS

Figure 1.12. Radiation patterns of LPHDA design "B"

end, however, the patterns held up quite well all the way to 800 megacycles

It is difficult to compare the boom length of design "B" with that of an LPD of the same directivity, because existing LPD design charts do not give complete figures for directivities lower than about 7.5 db. It is clear that the LPD would be somewhat shorter. It is also worthwhile to note that the insertion of τ and σ for design "B" into the LPD design charts gives a directivity of about 8.8 db.

In order to investigate the effect of Z_o, a new model (LPHDA-6) was built in which Z_o could be varied up to a maximum of 275 ohms. Design "B" was used for τ and σ. Impedance measurements, at different values of Z_o, showed a rather distinct improvement in VSWR at Z_o = 250 ohms, for which the impedance pattern is shown in Figure 1.13. The VSWR here is about 1.95. It increased to 2.33 and 2.31 at Z_o = 230 and 275 ohms, respectively. Pattern measurements showed results very similar to those obtained with Z_o = 100 ohms: the directivity was about 6.5 db, and the front-to-back ratio averaged 15.27 db from 400 to 800 Mc and 20.2 db from 514 to 800 Mc.

Measurements are now under way on another variable - Z_o model, patterned after design "B", but with a capability of Z_o values considerably higher than 250 ohms.

1.2.4 k-β Characteristics of Uniform Arrays

At any given frequency within the operating range of a log-periodic array, the active region of this array may be approximated by a uniformly periodic array of dipoles which are resonant at that frequency. Moving along the LP array, from the transmission region through the active region and into the unexcited region, is equivalent to changing the frequency of the signal applied to the LP array, from a frequency below dipole resonance to a frequency above dipole resonance. For this reason, LP arrays have been used extensively as laboratory models, especially for the study of k-β characteristics.

The k-β characteristic of a radiating periodic structure is a convenient way of relating the excitations of the radiating elements (in this case, the dipole currents) to the far-field radiation pattern of the structure. It has been studied extensively, both theoretically and experimentally.[10,11] Although its full meaning is not yet completely understood, it was felt that it would be of interest to obtain experimentally the k-β diagram for a uniformly periodic helical dipole array

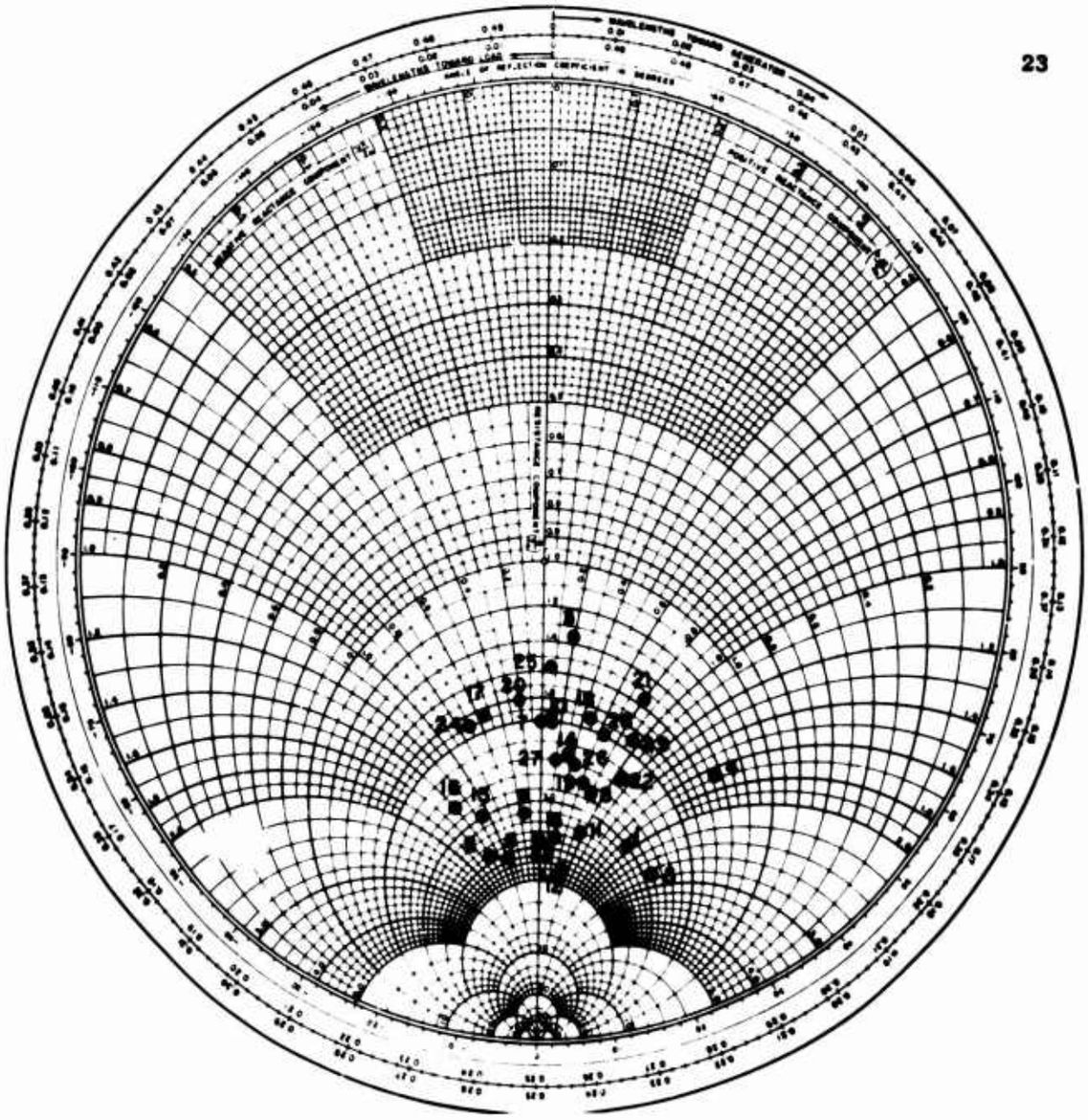

LPHDA-6a (s=0.54)

σ=0.07 τ=0.92

Z_o=250 Ω 400-800 Mc

Point	Freq.	Point	Freq.	Point	Freq.
1	400 Mc.	11	528 Mc.	21	698 Mc.
2	411	12	543	22	717
3	423	13	558	23	737
4	435	14	574	24	759
5	447	15	590	25	780
6	460	16	607	26	801
7	473	17	624	27	825
8	486	18	642	28	896
9	500	19	660	29	922
10	514	20	678		

Figure 1.13. Input impedance of LPHDA - 6a at optimum Z_o

(UPHDA) for purposes of comparison.

UPHDA-3, shown in Figure 1.14, was constructed for this measurement. It contained 14 identical dipoles, equally spaced with $\sigma = 0.087$ and $s = 0.53$. Appendix B discusses the method of probing the antenna so that the measured signal was proportional to the dipole currents. Relative amplitude and phase of the probe signal were measured at many frequencies as a function of distance along the feeder. Figures 1.15 and 1.16 show a representative sampling of the data obtained. The resulting k-β diagram, including attenuation vs. k, is shown in Figure 1.17.

The k-β diagram is often plotted in terms of ka vs. βa, where a is the "period" of the structure, i.e., the length of one "cell" or the distance from one dipole to the next. Here, $k = \frac{2\pi}{\lambda_o}$, the free-space phase constant, and $\beta = \frac{2\pi}{\lambda_g}$, the phase constant along the structure. Thus it is clear that plotting $\frac{a}{\lambda_o}$ vs. $\frac{a}{\lambda_g}$, as in Figure 1.17, is equivalent to plotting ka vs. βa except for a constant factor 2π. The $\frac{a}{\lambda_g}$ coordinate of each point was calculated by making a straight-line approximation to the phase curve at each frequency, wherever possible (for example, 300 Mc in Figure 1.15). The attenuation per cell was calculated by making a straight-line approximation to the amplitude curve. Not all of the phase curves could be translated into points on the k-β plot. For example, at 393 Mc (Figure 1.15) and at 1020 and 1040 Mc (Figure 1.16), straight-line approximations to the phase curves could not be made. This effect is common to such measurements, it can be caused by more than one mode being predominant on the structure at one time. For these frequencies, points were not plotted on the k-β diagram.

Figure 1.17 is similar in form to diagrams derived from measurements on arrays of linear dipoles. The one important difference is that the maximum value of attenuation per cell on the UPHDA is about 6 db, while values of 20 db or so have been obtained in arrays of linear dipoles. This important result agrees with the concept of a wider active region on the LPHDA, the effects of which were seen in UPHDA-1 (Section 1.2.1) and LPHDA-2 vs. LPD-2 (Section 1.2.2).

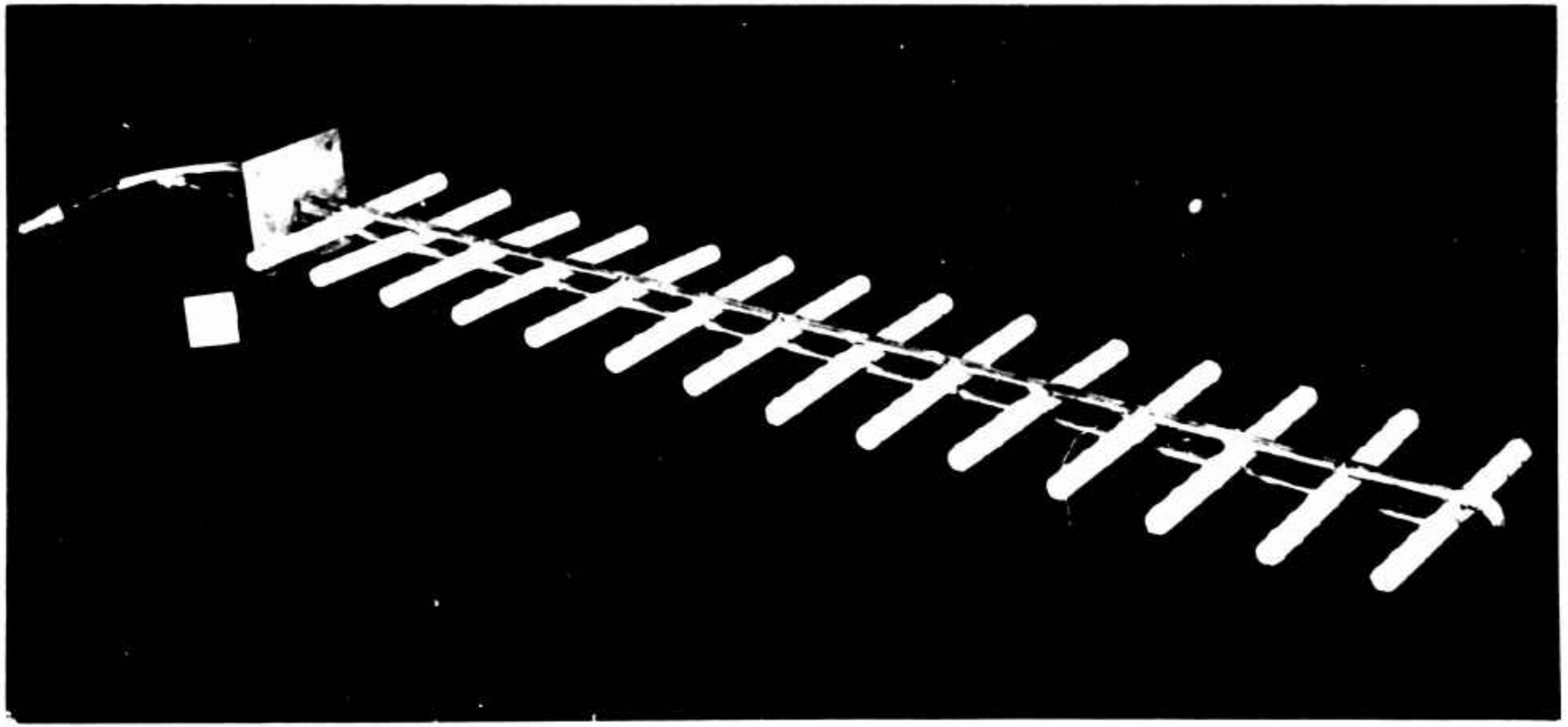

Figure 1.14. Laboratory model UPHDA - 3

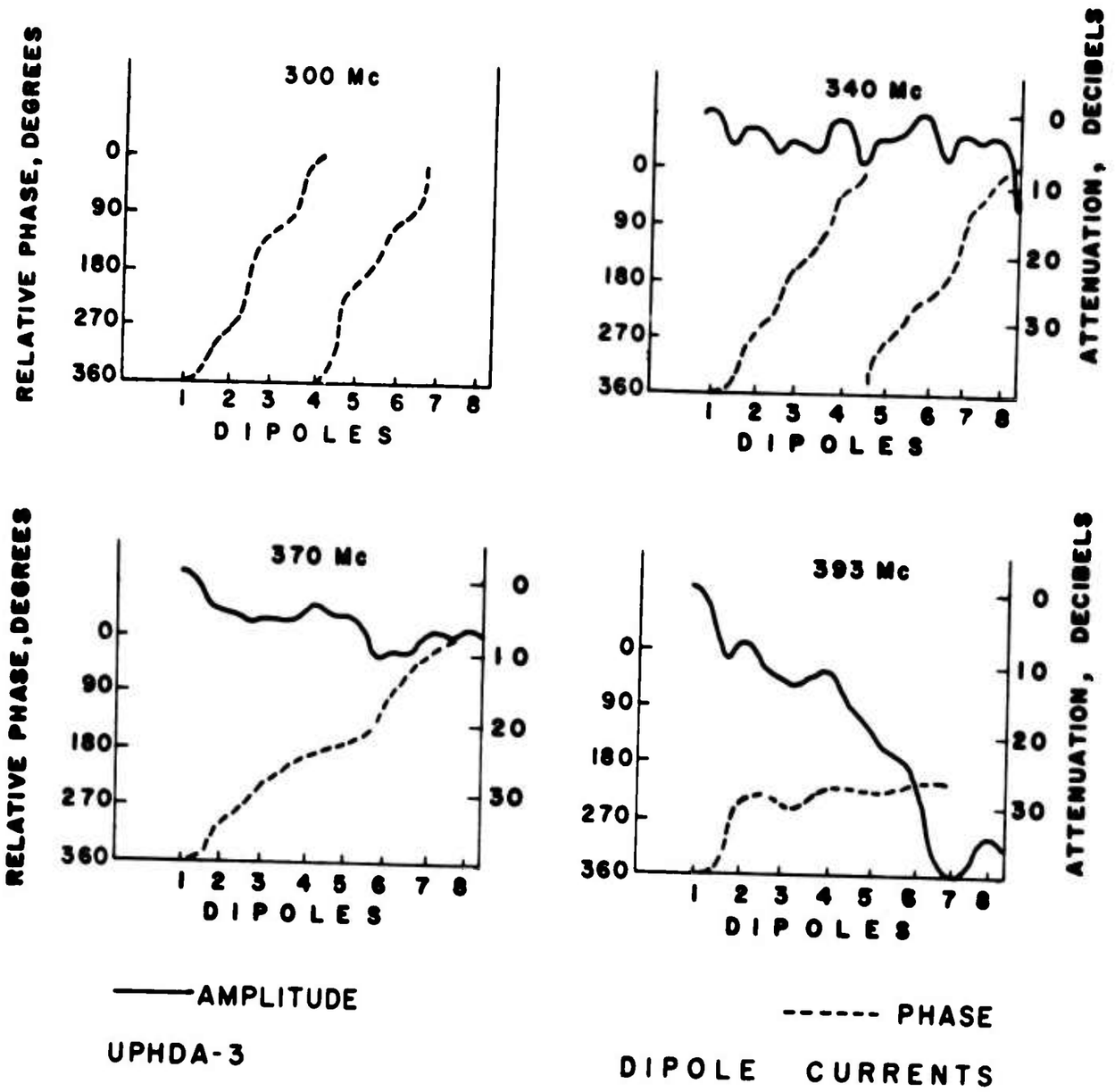

Figure 1.15. Data for UPHDA - 3 near first stop-band

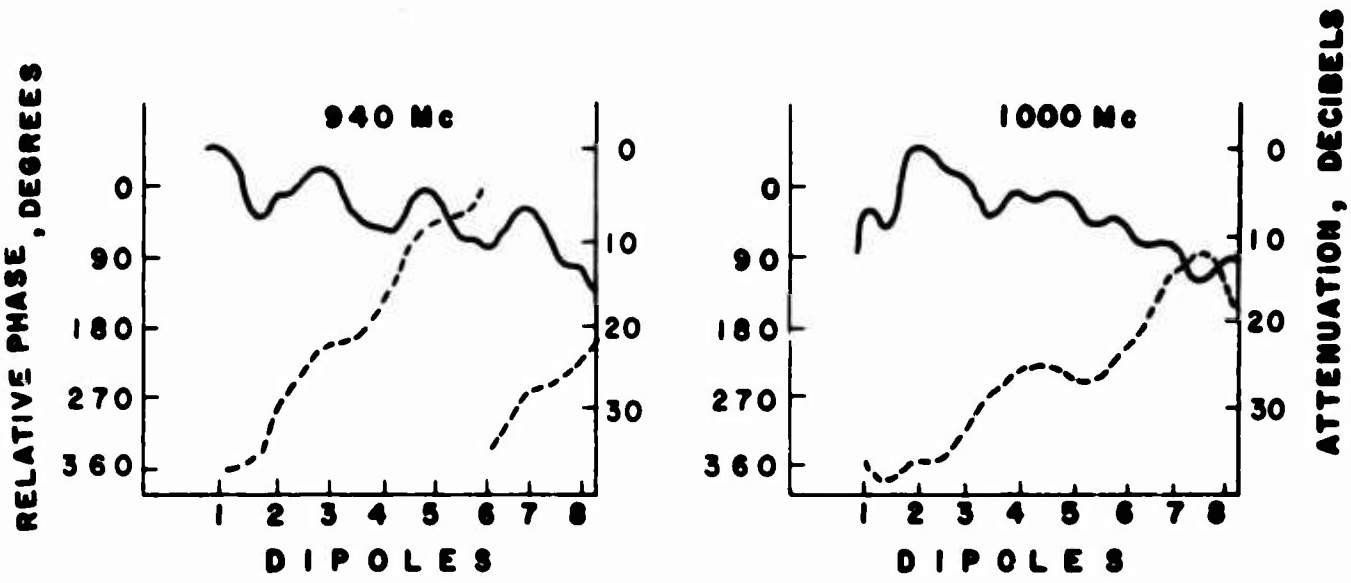

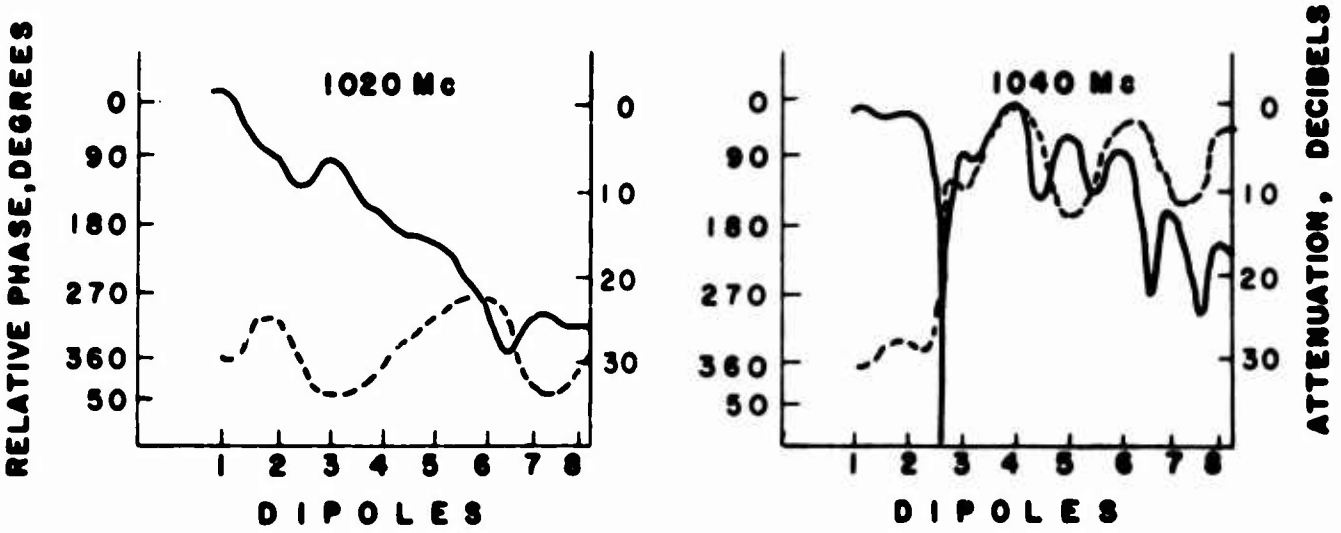

Figure 1.16. Data for UPHDA - 3 near second stop-band

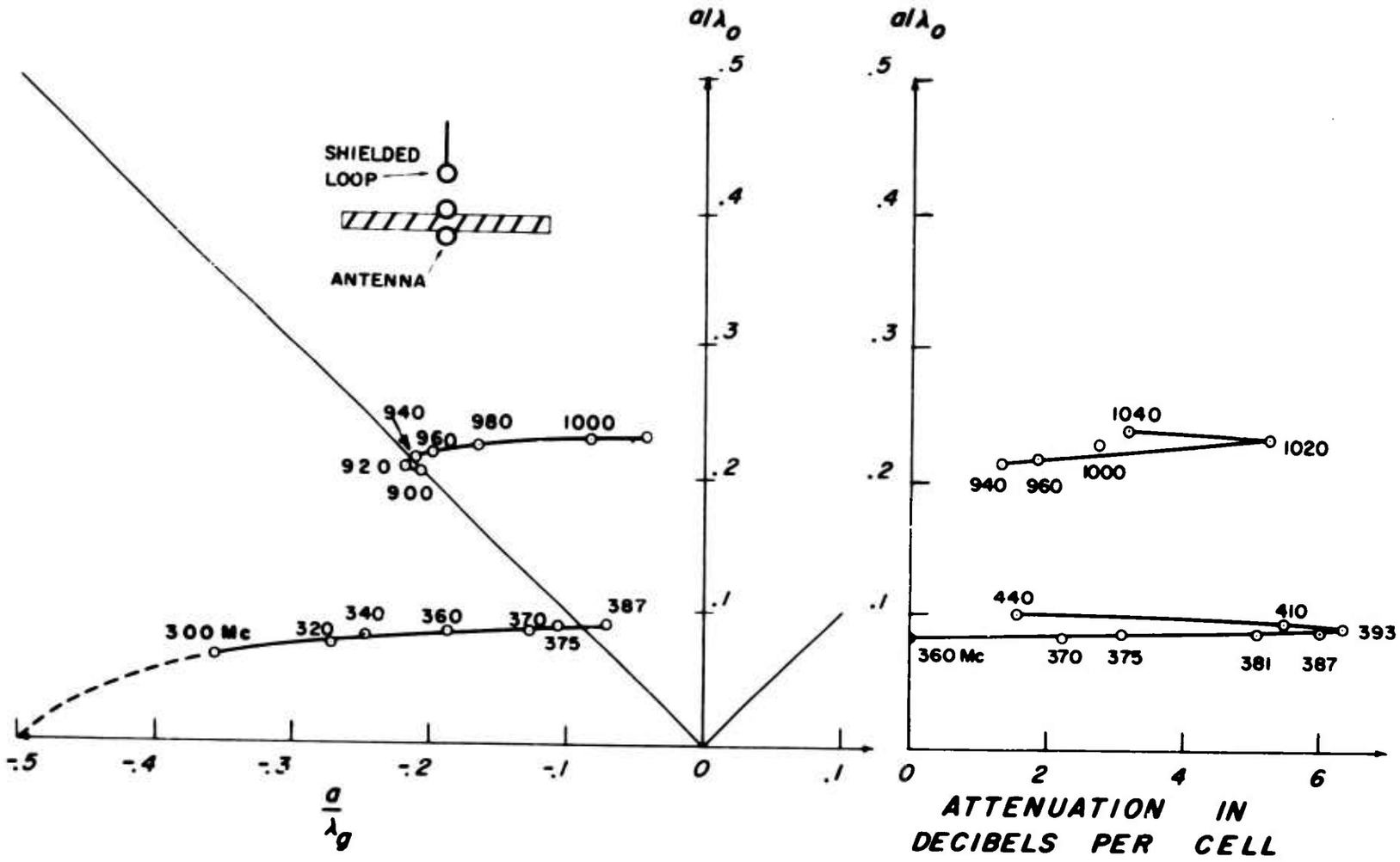

Figure 1.17. k-β diagram and attenuation per cell for UPHDA - 3

Measured far-field radiation patterns, shown in Figures 1.18 and 1.19 show excellent agreement with the k-β plot. The low values of attenuation per cell at 360, 800, 900 , and 920 megacycles produce the bidirectional form of the patterns at these frequencies, as was the case with UPHDA-1 with five dipoles. Maximum attenuation per cell in the first stopband occurs at k-β points fairly close to the backfire region. In the second stopband maximum attenuation does not occur until the beam has split considerably toward broadside. This, plus the fact that the second stopband occurs at a frequency less than three times the frequency of the first stopband, indicates that further study might be necessary to achieve good operation in the 3/2 wavelength mode.

Figure 1.18 shows calculated patterns in addition to the measured ones at 375 and 393 megacycles. These calculations were based on the measured dipole current amplitudes and phases, in an attempt to evaluate the accuracy of these measurements. The results indicate an acceptable degree of reliability for the measured data. It should be remembered that the pattern measurements, taken on existing facilities at the Antenna Laboratory, are most accurate at frequencies above 500 megacycles.

1.3 Log-Periodic Mixed Dipole Arrays

In the preceding sections, the work described was devoted to optimizing the performance of an LPHDA. This section describes the investigations of a more practical design, which combines the size reduction of an LPHDA with the performance of an LPD. The log-periodic mixed dipole array (LPMDA) is based on the idea that in a broadband antenna the need for size reduction is felt most strongly in the longer (lower-frequency) dipoles only, the shorter dipoles may just as well be linear ones. Over most of the frequency range, then, the antenna would perform with the higher directivity and more uniform impedance characteristics of an LPD, and the sacrifice in performance inherent in an array of helical dipoles would be felt only in the first few log-periods at the low-frequency end of the band.

Figure 1.20 is a photograph of the two mixed arrays that were built and tested. These models are 1/70-scale models of 6-25 megacycle arrays (frequency range for models: 420-1750 Mc). The first four dipoles on each model are helical, the rest are linear. Unlike in previous models, the helical dipoles are not scaled in length. For the first dipole, s = 0.5, for the second, third, and fourth dipoles, s increases to $0.5\,\tau^{-1}$, $0.5\,\tau^{-2}$, and $0.5\,\tau^{-3}$, respectively. Thus all four helical dipoles are the same length, but s is adjusted for each so that the resonant

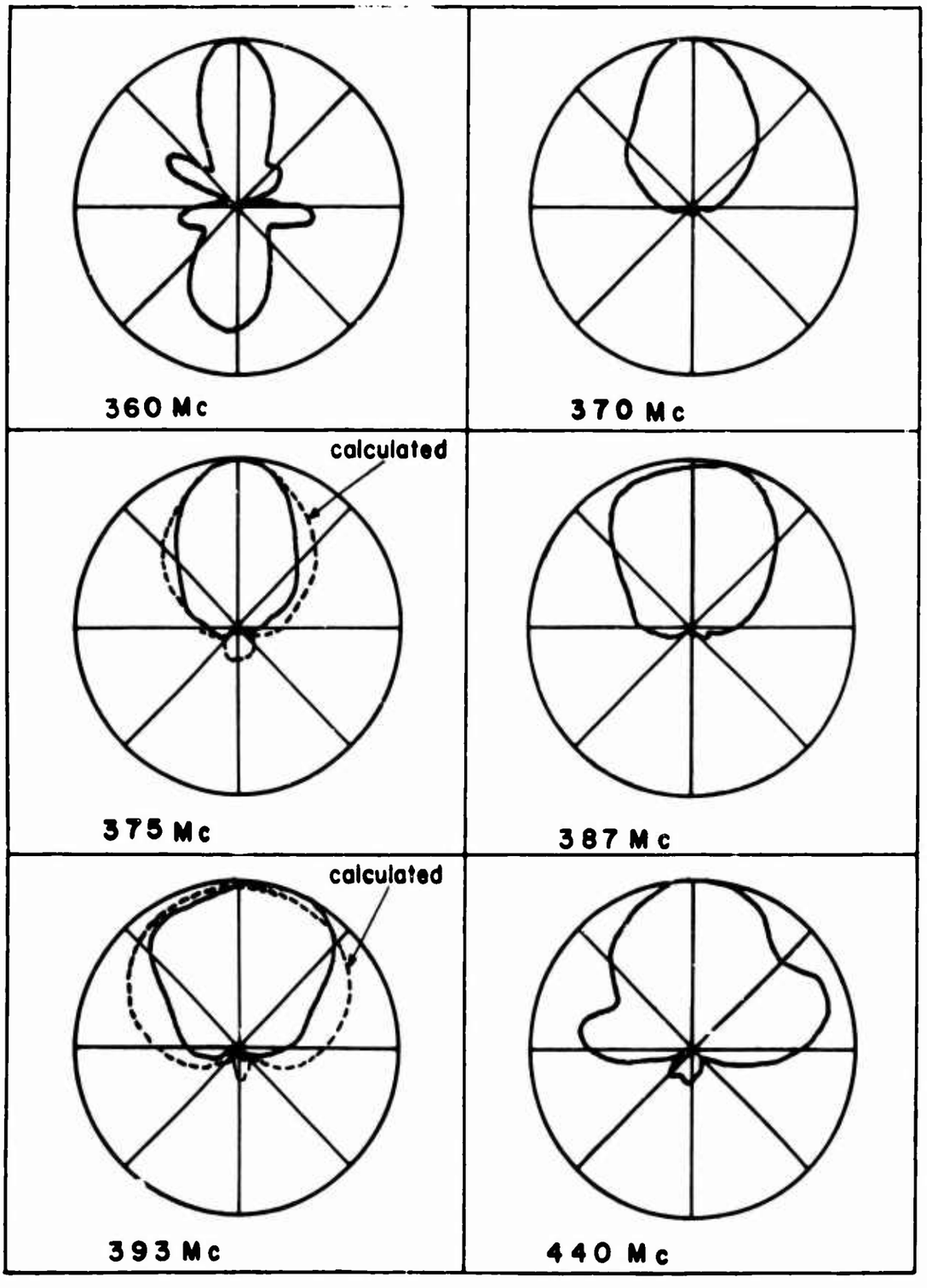

Figure 1.18. Radiation patterns of UPHDA - 3 near first stop-band

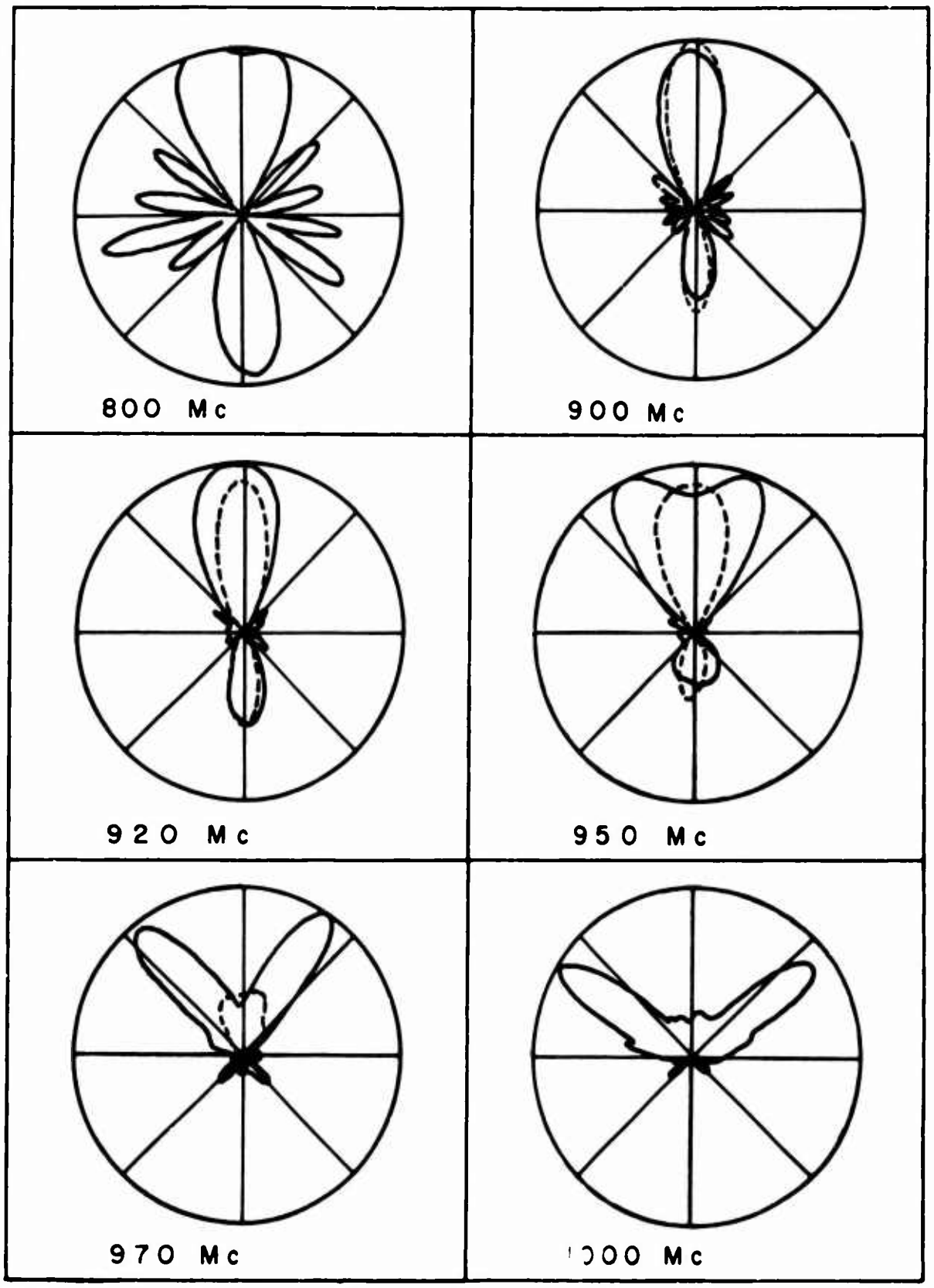

Figure 1.19. Radiation patterns of UPHDA - 3 near second stop-band

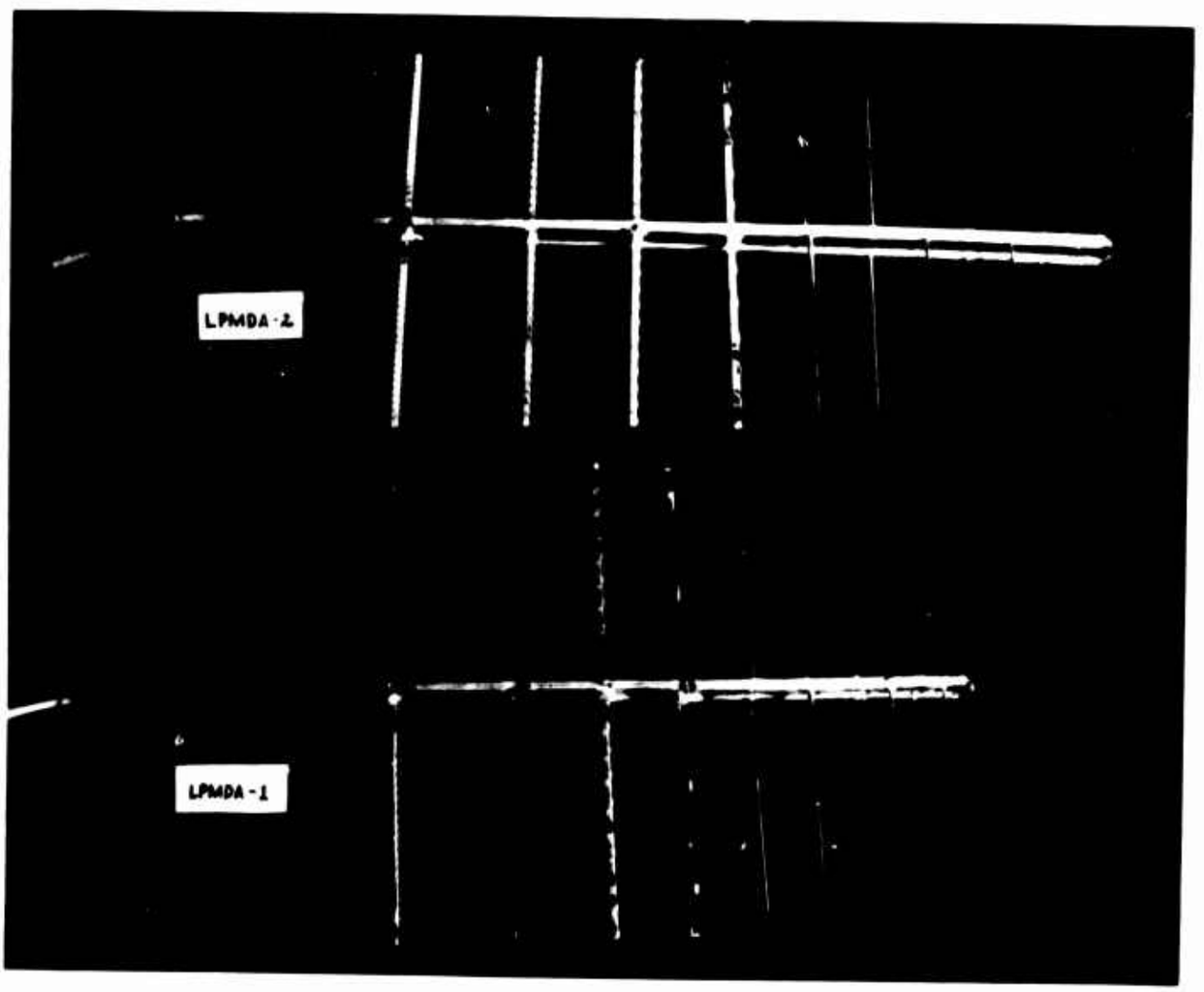

Figure 1.20. Laboratory models LPMDA - 1 and 2

frequencies scale log-periodically from one to the next. This provides, in effect, a gradual transition from helical to linear dipoles.

Other design parameters were:

LPMDA-1. $\tau = 0.825$, $\sigma = 0.06$, $\alpha = 36^{o}$, $Z_o = 135$

LPMDA-2. $\tau = 0.85$, $\sigma = 0.07$, $\alpha = 28^{o}$, $Z_o = 135$

These are far from the optimum parameters found for the LPHDA; they were chosen to represent a useful and reasonably compact LPD design.

Impedance measurements resulted in data such as shown for LPMDA-1 in Figure 1.21. The sixteen points shown are spaced evenly through the first four log-periods. The point labelled "f_1" is at the resonant frequency of the first helical dipole; the next three points connected to it by the line correspond to frequencies $\tau^{-1/4} f_1$, $\tau^{-1/2} f_1$, and $\tau^{-3/4} f_1$. The next point is the one labelled "f_2", etc. It will be noticed that as frequency is increased the impedance pattern, with the exception of the point labelled "f_4", spirals inward towards a progressively lower VSWR. Impedance points at frequency f_5 and above are omitted for clarity, but they are clustered around the point 1.5 + j 0 with a VSWR of less than 2.

Figure 1.22 shows some of the radiation patterns of this same antenna. Again, with the exception of the H-plane pattern at f_4, performance improves progressively as frequency is increased; this time in terms of directivity and front-to-back ratio (note particularly the E-plane patterns). Above frequency f_5, the pattern remained quite uniform.

These results may be summarized as follows:

Freq Range	VSWR	Front-to-Back Ratio
$f_1 - f_2$	3.58	3.36 db
$f_2 - f_3$	2.27	8.22 db
$f_3 - f_4$	2.11	11.69 db
$f_4 - f_5$	1.91	20.28 db
f_5 and above	1.91	21.5 db minimum

The impedance and pattern at the single frequency f_4 are omitted from the above table. This seems to be an exceptional point, data at all other frequencies were well-behaved.

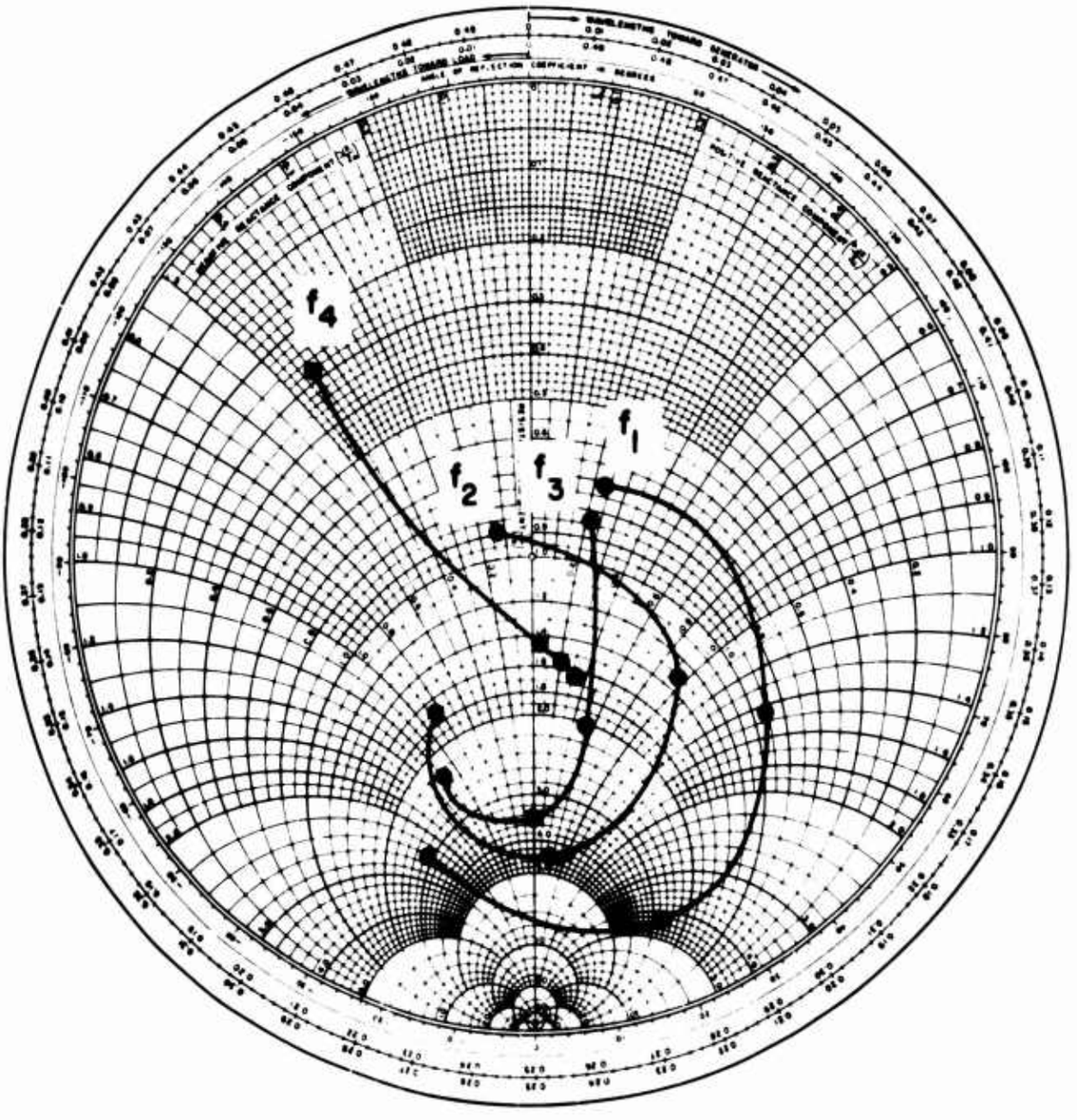

LPMDA-1: FIRST FOUR LOG-PERIODS

$\sigma = 0.06$ $\tau = 0.825$ $\alpha = 36°$

Figure 1. 21. Input impedance of LPMDA - 1

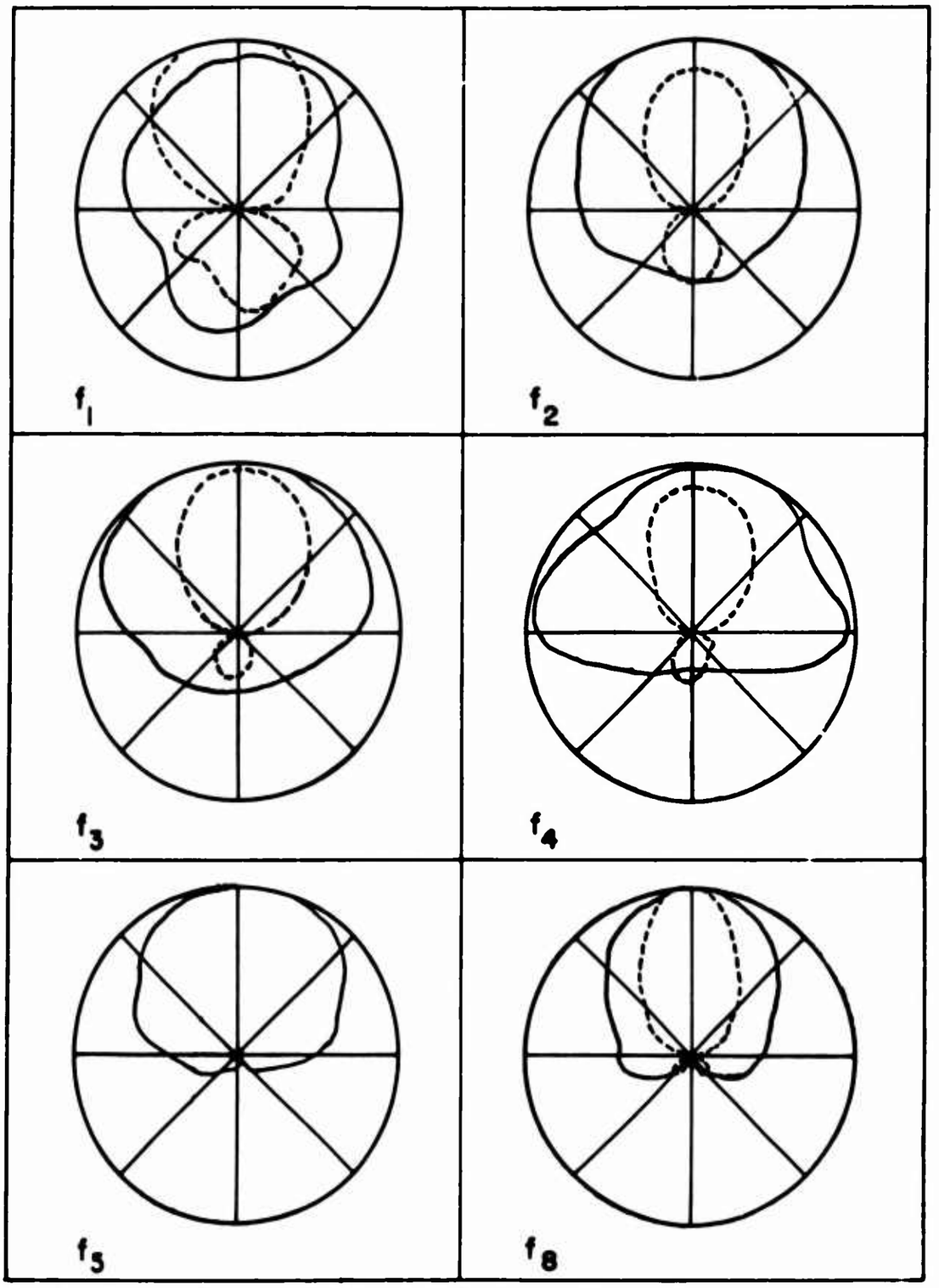

Figure 1.22. Radiation patterns of LPMDA - 1

Model LPMDA-2 behaved in a manner very similar to that of LPMDA-1. In evidence again was the gradual improvement in performance as frequency was raised toward the range where the linear dipoles become active.

It is appropriate here to comment on the idea of overall size reduction, i.e., the effect of the 50% shortening upon the diameter of a clear circular area which would be required to allow the antenna to be mounted horizontally and rotated in azimuth. A 6-25 Mc log-periodic dipole array, built according to the values of τ and σ that were used in LPMDA-2, would require a circular area 28.2 meters in diameter. With dipole shortening of 50% on the first dipole, etc., as was done in LPMDA-2, the diameter of the required area reduces to 22 meters, an overall size reduction of 0.78. The same analysis, applied to arrays with τ and σ as used in LPMDA-1, results in a diameter of 25.6 meters for the LPD array, and 17.6 meters for the mixed array, an overall size reduction of 0.6875. These reductions, of course, are based on design parameters that are better suited for linear dipole arrays than for helical dipole arrays. A similar analysis performed on arrays built according to, say, design "B" of Section 1.2.3 would result in considerably higher value for overall size reduction.

Two methods are proposed, whereby the low-frequency performance of LPMDA antennas might be improved. The first method consists of raising τ and decreasing σ for the helical elements only. This could be done in such a way as to cause little or no change in the overall size reduction described above, but the degree of improvement might be limited. The change in parameters could be made gradually, as s was changed gradually, or it could be made all at once at the point where the helical dipole section and the linear dipole section come together. Further experiments would be needed to determine to what extent the operating characteristics of the antenna could be kept uniform throughout its frequency range.

The second possible method of improving LPMDA performance is actually one that was suggested by the results of Section 1.2.2: add an extra dipole to the low-frequency end of the antenna, i.e., design the antenna for a low-frequency cutoff one log-period below the lowest frequency at which the antenna will be used. This method, of course, lengthens the array and adversely affects the overall size reduction.

To provide an idea as to the effectiveness of this procedure, LPMDA models 1 and 2 were both measured for impedance with their first helical dipoles removed.

In each model, the resulting VSWR was higher, frequency for frequency, than for the original array. For example, while the original LPMDA-1 measurements resulted in a VSWR of 2.27 from f_2 to f_3, the new data gave 2.77 for the same frequency range and 2.26 for the range f_3 to f_4. In general, the performance of the array with one dipole deleted was similar to that of the original array at a frequency range one log-period higher.

1.4 Usefulness of Size-Reduced Arrays; Practical Design Considerations

1.4.1 Summary of Data and LPHDA and LPMDA Uses

Results of the data obtained in this investigation may be summarized as follows:

A. Helical dipoles are useful and practical size-reduced elements for use in a log-periodic array. It is advisable, however, to measure the resonant frequency of at least one dipole from any given array, and to adjust its resonant frequency experimentally to the desired value. The rest of the dipoles in the array may then be designed by scaling all dimensions from those of the measured dipole by powers of τ.

B. The substitution of helical dipoles for linear ones in an LP array leads to higher VSWR and poorer directivity. Any given set of design parameters for an LPHDA produces an antenna whose boom length is greater than that of an LPD of comparable performance.

C. The active region on an LPHDA is wider (contains more dipoles) than that of an LPD array. Consequently the operating bandwidth of the LPHDA is narrower. This effect occurs principally at the low-frequency end.

D. Perhaps the most practical design for an antenna with a very large bandwidth is the log-periodic mixed dipole array.

From these characteristics, several conclusions may be drawn concerning possible ways in which LPHDA or LPMDA antennas may be of value. An antenna designer who is faced with space limitations may find such an array to suit

his needs if he is willing to give up bandwidth. If he needs large bandwidth, these designs may still be useful if he is willing to sacrifice shortness by adding an extra log-period or two to the low-frequency end. Or perhaps his problem is one of mechanical support or rigidity: a long boom on which are mounted long dipoles could be quite difficult to support rigidly on, say, the top of a tall mast. Shortened, stiffer dipoles have an obvious advantage here, even if using them means making the boom longer.

1.4.2 Practical Design Considerations

Once the decision is made to use an LPHDA or LPMDA, some comments are needed concerning the construction of a low-frequency model — one, for example, which would operate in the HF (3-30 Mc) range.

Two important helical dipole parameters are the ratio of helix diameter ("D" in Figure A-2) to length or to free-space wavelength, and the ratio of wire diameter to helix diameter. The choice of these ratios is somewhat limited: If D is too small, the dipole will be too flexible and will require excessively small wire. But if D is too large, the dipole is bulky and heavy, and it will produce a strong cross-polarization component in its radiation field. For a given helix diameter, wire which is too small will create high resistive losses; large wire adds weight, makes the helix core smaller and therefore weaker, and does not give as low a value of S as does a smaller wire, wound to the same diameter and pitch. Laboratory models have featured wire size-to-helix diameter ratios between 0.1 and 0.02, and helix diameter-to-length ratios of 0.1 to 0.04. Within these limits, the specific ratios chosen are not critical.

Polystyrene was chosen for the helix core material in laboratory models because of its low loss at the high frequencies used for testing the models. For low-frequency antennas, fiberglass is a widely used material, and would be an excellent choice for helical dipoles As long as the helix diameter is quite small compared to its length, the performance of the dipole is affected very little by the dielectric properties of the core material; therefore it would not matter electrically whether the core is made hollow or solid. A hollow fiberglass core would probably be both light and sufficiently strong. For the helix wire, any good conductor could be used. Copper tubing is a common material for large-diameter conductors. It need not have a round cross section. a strip of thin sheet material could be used instead of wire or tubing.

In any case, once the materials and parameters are chosen for an LPHDA and a dipole built and measured, it is important that length, diameter,* pitch, and conductor size are all scaled by the factor τ from one dipole to the next in order that the resonant frequency will be scaled by τ also. This is not the case, however, for the LPMDA, on the models shown in Figure 1.20, only the pitch was scaled. Dipole length, diameter, and wire size remained constant for all four helical dipoles. To achieve the proper dipole resonant frequencies, it was found necessary to build several dipoles of different pitch, plot their resonant frequencies as a function of pitch, connect the points with a smooth curve, and then read from the curve the values of pitch needed to give the proper resonant frequencies for each of the dipoles.

Construction of the feeder on an LPHDA or LPMDA is no different from the construction of conventional LPD feeders in the same frequency range. The method of securing the dipoles mechanically to the feeder will be determined by the materials used, the strength required, and the relative sizes of the pieces to be joined together. The presence of a piece of dielectric (the helix core) in and around the feeder at each dipole location will not have an appreciable effect on the operation of the feeder, so long as the cores are not excessively large.

1.4.3 Future Work, Conclusions

Research performed on this task to date has indicated a number of areas in which further work is necessary. Some of these areas were mentioned earlier in the report: the effect of the feeder impedance Z_o, and the optimization of LPMDA performance in the helical dipole region by changing τ, σ, and Z_o. Studies of the UPHDA k-β characteristics suggest that it might be possible to increase the gain by inserting extra phase shift in the feeder between dipoles. A mathematical analysis, similar to those performed by Carrel[3] or Mittra and Jones[11], could help in understanding the performance of LPHDA antennas and provide useful data for design charts. New facilities to be obtained for the Antenna Laboratory will permit measurements of absolute gain, and thus of overall efficiency.

The authors feel that the present work, together with work on the above items in the coming year, will make the log-periodic helical and mixed dipole arrays useful members of the popular family of frequency-independent antennas.

---

* Diameter D, as used in this report, is the diameter of the helical path described by the center of the wire. It is equal to the core diameter plus twice the wire radius.

REFERENCES

1. V. H. Rumsey, "Frequency - Independent Antennas", Technical Report No. 20, Antenna Laboratory, University of Illinois, Contract AF 33(616)-3220, 25 October 1957.

The geometry of antennas specified by angles is presented. Observations are made on the theory of convergence of patterns and impedances to frequency - independent values. Appendix discusses surfaces for which a rotation is equivalent to an expansion.

2. Dwight E. Isbell, "Log-Periodic Dipole Arrays", Technical Report No. 39, Antenna Laboratory, University of Illinois, Contract AF 33(616)-6079, 1 June 1959.

The LPD is described, together with a brief note on its evolution from other structures. Results are given of measurements of the truncation effect, input impedance, radiation patterns,and bandwidth in terms of the lengths of the longest and shortest dipoles.

3. R. L. Carrel, "Analysis and Design of the Log-Periodic Dipole Antenna", Technical Report No. 52, Antenna Laboratory, University of Illinois, Contract AF 33(616)-6079.

Presented here is a complete history of antenna designs leading up to the LPD. The antenna is anlayzed mathematically for input impedance, patterns, etc., and its operation is described thoroughly. A complete set of design data is given, including examples and the results of measurements on models built from these data. An appendix discusses measurement techniques.

4. H. A. Wheeler, "A Helical Antenna for Circular Polarization", Proc. I.R.E., Vol. 35, p. 1484, December 1947.

The far-field radiation pattern of a short helical dipole is studied, with particular interest to the condition on coil area and pitch which produces circular polarization. Discussed also is the use of multifilar helices to raise power factor and efficiency. Circuit connections to a receiver or transmitter are discussed.

5. J. D. Kraus, Antennas, Chapter 7, page 173, McGraw-Hill, 1950.

In this well-known text, helical antennas are thoroughly studied. A unified treatment explains similarities and differences between normal-mode and axial-mode helical antennas. Radiation patterns and polarizations are studied. Most of the chapter is devoted to axial-mode antennas.

6. A. G. Kandoian and A. Sichak, "Wide-Frequency-Range Tuned Helical Antennas and Circuits", Electrical Communication, Vol. 30, p. 294, December 1953. Also Convention Record, I.R.E. National Convention, 1953, part 2, p. 42.

This reference describes the use of a helix as a distributed circuit element to reduce size, also the use of normal-mode helical dipoles instead of short linear dipoles. Equations are given for axial velocity of propagation, radiation resistance, polarization, losses, "Q", and tap point for circuit connections. Circuit applications include delay lines and wide-range

resonant elements. The design charts for helical dipoles are reproduced in "Reference Data for Radio Engineers", page 682, published by the International Telephone and Telegraph Corporation.

7. Tingye Li, "The Small-Diameter Helical Antenna and Its Input Impedance Characteristics", Ph.D. Thesis, Electrical Engineering Department, Nortwestern University, June 1958.

A mathematical analysis is given of the input impedance of a normal-mode helical dipole. Radiation characteristics are studied. The use of folded helical dipoles and dipoles with varying pitch is discussed.

8. L. J. Chu, "Physical Limitations of Omnidirectional Antennas", Journal of Applied Physics, Vol. 19, page 1163, December 1948.

Using spherical wave functions to describe the radiated field, a study is made of gain and "Q" of an arbitrary antenna. Three criteria are used for optimum performance: maximum gain for a given complexity, minimum "Q", and maximum ratio of gain divided by "Q". Practical limitations are also discussed.

9. H. A. Wheeler, "Fundamental Limitations of Small Antennas", Proc. I.R.E., Vol. 35, p. 1479, December 1947.

A study is made of an inductor and a capacitor acting as small antennas. Length is less than $1/2\pi$ wavelength. Formulas are given for capacitance, inductance, susceptance, reactance, radiation conductance or resistance, radiation power factor, coupling and circuit efficiencies when connected to tuned circuits. Examples of applications include small radio receiver loops, short wires, loops in TV and FM cabinets.

10. P. E. Mayes, G. A. Deschamps, and W. T. Patton, "Backward-Wave Radiation from Periodic Structures and Application to the Design of Frequency-Independent Antennas", Technical Report No. 60, Antenna Laboratory, University of Illinois, Contract AF 33(657)-8460, April 1963.

The theory of radiation from periodic structures is discussed. Applications are made to monopole and dipole arrays, zig-zag antennas, and the backfire bifilar helix.

11. R. Mittra and K. E. Jones, "Theoretical Brillouin (k-β) Diagram for Monopole and Dipole Arrays and Their Application to Log-Periodic Antennas", Technical Report No. 70, Antenna Laboratory, University of Illinois, Contract No. AF 33(647)-10474, April 1963.

The characteristic equation for the complex propagation constant of a dipole-loaded transmission line is derived. A solution is obtained; the effects of mutual impedances are included. The results are compared with experimental results by Mayes and Ingerson. The usefulness of the k-β diagram for analyzing LP structures is discussed.

APPENDIX A

DESIGN OF HELICAL DIPOLES

An exact mathematical solution does not yet exist for a normal-mode helical dipole wound with fairly large wire. Existing studies on this subject deal with such approximating structures as the sheath or tape helix, or the helix wound with very small wire. Therefore an experimental approach is the most suitable method for predicting the resonant frequency of a helical dipole to the degree of accuracy needed in order to use the dipole in a log-periodic array (or, for that matter, as a narrow-band antenna for single-frequency use).

This appendix illustrates the parameters used to describe a helical dipole. As an aid to experimental design, data from helical dipole measurements are presented to show in a general way the extent to which changes in certain design parameters affect resonant frequency and shortening factor.

A.1 Helical Dipole Design Parameters

Figure A-1 illustrates a helical dipole of length 2 h, wound with circular cross section wire of diameter 2a onto a cylindrical core of diameter d. The mean helix diameter, D, is the same as that referred to in Figure 2 and in the footnote in Section 1.4.2. The pitch of the helix is denoted by p. Certain other relationships are easily derived from Figure A-1; for example,

$$N = \text{number of turns} = \frac{2h}{p}$$

$$\psi = \text{pitch angle} = \arctan\frac{p}{\pi D}$$

Figure A-1 does not show the feed point of the dipole. To provide a feed point, the wire is cut at the center of the dipole, $\frac{N}{2}$ turns from either end. Just enough wire is unwound, in equal amounts from each half of the dipole, to make the necessary circuit connection. In practice, of course, one may wind the dipole with two separate pieces of wire instead of using one wire and then cutting it. The portion of a turn at the dipole center which is unwound for the circuit connection should be as small as possible.

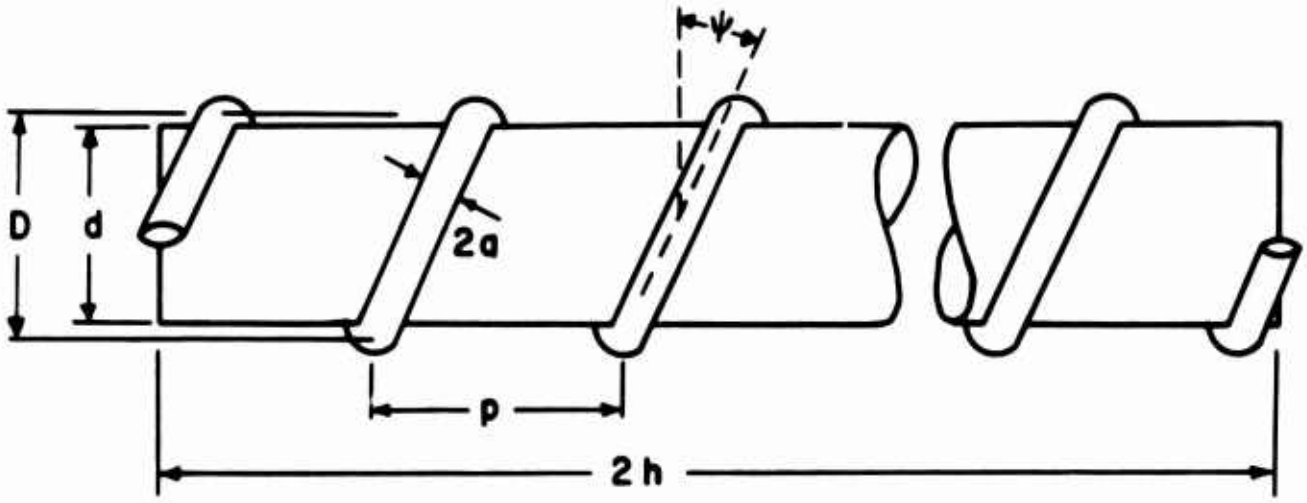

Figure A-1. Parameters of a helical dipole

A.2 Results and Applications of Dipole Measurements

Thirty-six dipoles were built and their resonant frequencies measured. The parameters $\frac{p}{D}$, $\frac{D}{2h}$, and $\frac{2a}{D}$ were varied, but the dipole length 2h was held constant at 18 centimeters for all dipoles. Since an 18-centimeter linear dipole resonates at 833 megacycles, the resonant frequency measured on a given helical dipole divided by 833 equals the value of s for that dipole.

In Figure A-2 are plotted the resonant frequencies and values of s as a function of the ratio $\frac{p}{D}$ for all of the dipoles measured. Each of the three graphs is for a different value of $\frac{D}{2h}$, and the three curves in each graph are for three different wire sizes ($\frac{2a}{D}$ ratios).

As an example of a way in which this data can be used, suppose that an antenna designer wants a helical dipole for a given resonant frequency and a given value of s. Using, for example, the data in Kandoian and Sichak[6], he determines the proper value of pitch to go with his chosen length 2h. He then measures its resonant frequency. If it is quite close to the desired value, he may be able to adjust it satisfactorily by shortening or lengthening the dipole slightly. Then his value of s would be a little different from the intended value. But if the measured frequency is quite far from the desired value, and he is reluctant to change 2h and settle for a different s, he can look for a curve in Figure A-2 which represents a value of $\frac{2a}{D}$ and $\frac{D}{2h}$ close to the value he is using, and get from it a new value of $\frac{p}{D}$ to try.

It was stated in Section 1.1.1 that to a first approximation the wave is assumed to travel along the wire with the velocity of light. This is the same as saying that $s = \sin \psi$. The dashed curve in the first graph of Figure A-2 shows how rough this approximation is. This curve is a plot of the equation resonant frequency = 1090 $\sin \psi$ Mc where the constant 1090 was chosen arbitarily (it makes the curve agree with the $\frac{2a}{D}$ = .1135 curve at $\psi = 30^{\circ}$).

Each graph of Figure A-2 shows how resonant frequency changes with wire size, and the three graphs taken together show how resonant frequency changes with helix diameter. Figure A-3, however, is designed to give a clearer picture of these changes. In Figure A-3a, frequency is plotted against wire size ($\frac{2a}{D}$) for a value of pitch ($\frac{p}{D}$) which gives shortening factors in the neighborhood of 0.5. The range of wire sizes used here is fairly small; earlier measurements performed on helical monopoles with a 10-to-1 range in wire diameter showed that resonant frequency was

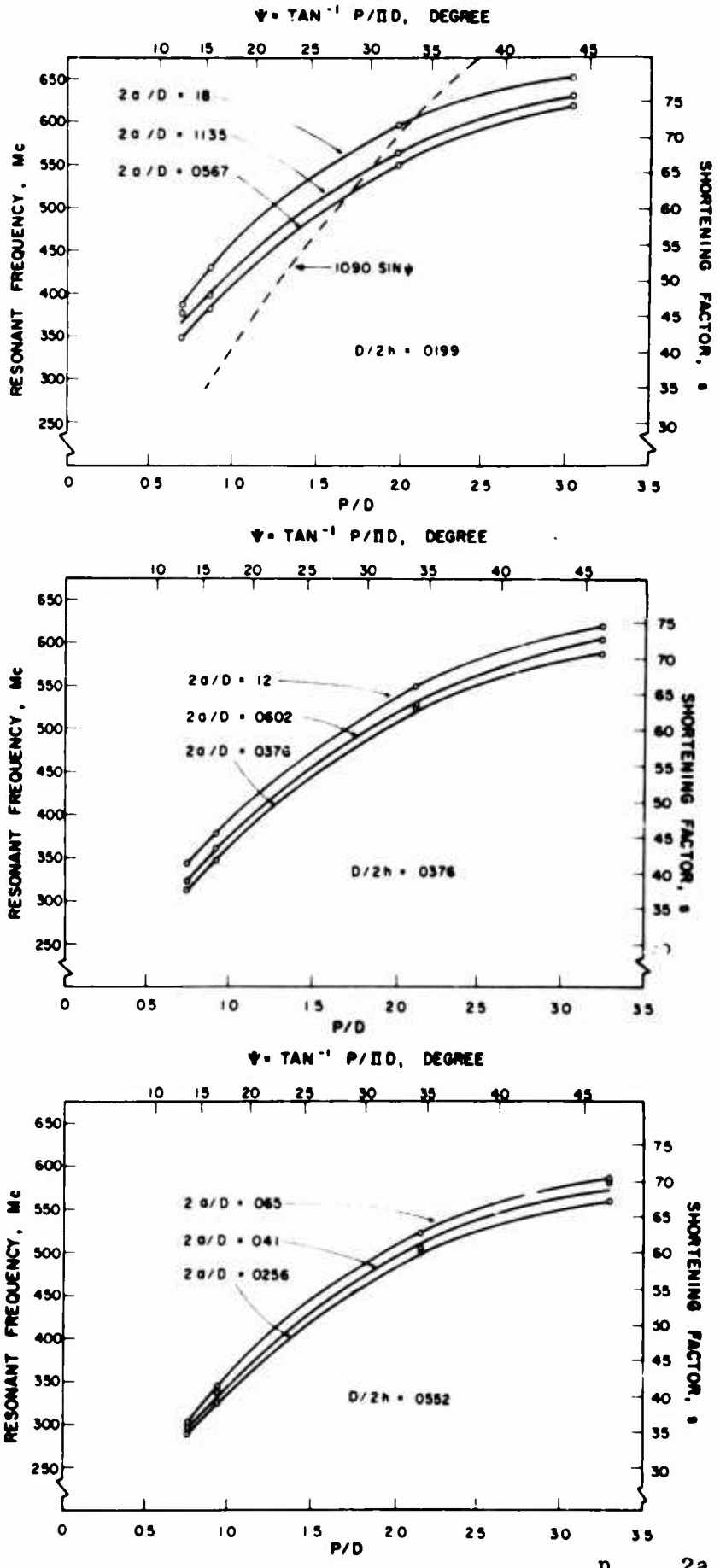

Figure A-2. Resonant frequency and shortening factor vs. $\frac{p}{D}$ and $\frac{2a}{D}$ for three values of $\frac{D}{2b}$; 2h = 18 cm = one-half wavelength at 833 Mc

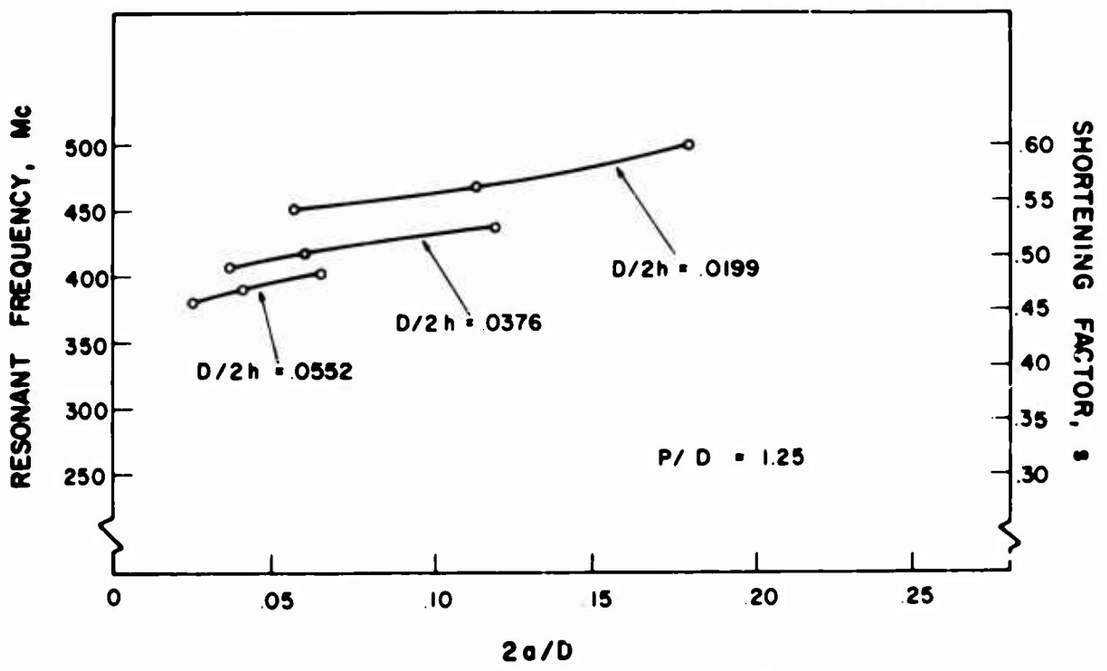

Figure A-3a. Resonant frequency and s vs. wire size; $\frac{P}{D}$ chosen for s in the neighborhood of 0.5

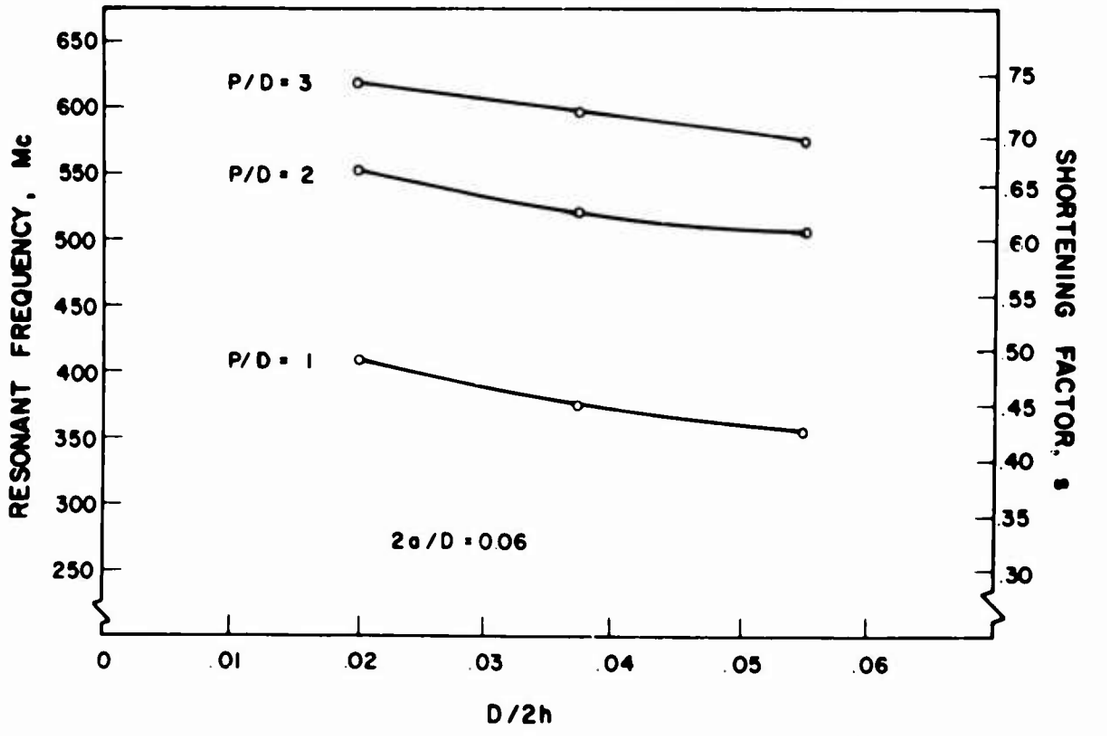

Figure A-3b. Resonant frequency and s vs. helix diameter for $\frac{2a}{D}$ = 0.06

proportional to the logarithm of the wire diameter. In Figure A-3b is shown the effect of helix diameter on resonant frequency for a constant ratio $\frac{2a}{D}$. Both of these sets of curves were derived from the curves of Figure A-2. They may be summarized by saying that increasing $\frac{D}{2h}$ or decreasing $\frac{2a}{D}$ leads to a smaller shortening factor.

Figure A-3b implies that the presence of dielectric with $\epsilon_r > 1$ inside the helix may help in slowing the wave propagating along the helix, thus contributing to dipole length reduction. Indeed, the presence of such a dielectric in a transmission line has just this effect; dielectric loading is often used for this purpose. Li[7] states that the presence of dielectric with $\epsilon_r \neq 1$ inside a very thin helix has essentially no effect on the guide wavelength in the helix. It is doubtful that the helices used in these tests could be called "very thin". In any case, it is quite possible that the use of a hollow core, which was impractical in the laboratory models used here, could reduce the effect of $\frac{D}{2h}$ on resonant frequency.

It is felt that further study could provide much more insight into the effects of helix parameters and materials on helical dipole performance. In the meantime, however, experimental techniques will continue to play an important part in the design of helical antennas.

APPENDIX B

MEASUREMENT TECHNIQUES

B.1 General

Data of the type presented in this report were obtained through laboratory measurements of the following four types of quantities: (1) relative phase of the near field, (2) relative amplitude of the near field, (3) input impedance referred to the antenna feedpoint, and (4) far-field radiation patterns. In this appendix are discussed the techniques by which these measurements were performed.

The range of frequencies for which antenna models were constructed and measured was limited by several factors. A Rohde and Schwarz Diagraph was used for impedance and phase measurements; its lowest operating frequency is 300 megacycles. The Antenna Laboratory's pattern range facilities give their most dependable performance at frequencies above 500 Mc (although new facilities are being obtained for lower-frequency work). The construction of accurately scaled helical dipoles is difficult for resonant frequencies much above 1000 Mc. Models of large bandwidth are desirable where "frequency-independent" antennas are concerned, because only in this way can one get away from end effect and into a reasonably large frequency region where performance is uniform. In previous work on log-periodic dipole arrays, two models of each design had often been built; one for impedance measurements, characterized by large, good-quality feed cables and a lower frequency range; the other for pattern measurements, scaled down in size and up in frequency from the impedance model. This was impractical for the LPHDA models, for two reasons: the much greater amount of time necessary to build each model, and the difficulty of scaling individual dipoles accurately with standard wire sizes. Therefore the impedances and patterns for each set of design parameters were taken on the same model, and a compromise frequency range was used.

For these reasons most of the LPHDA models were built with a lower frequency limit of 400 or 420 Mc, and an upper frequency limit of 800 to 1200 Mc. The uniformly periodic array used for near-field probing (UPHDA-3) was built with a resonant frequency of about 385 Mc.

B.2 Near-Field Phase Measurements

Relative phase (and amplitude) of the near-field signal on the uniformly periodic array were measured by two different methods of probing. In the first, the voltage distribution on the antenna feeder was sampled, using a short, straight wire probe sensitive to the electric field between the two halves of the feeder. This

probe, together with a small polystyrene spacer, is visible in Figure 1.14 between the first and second dipoles. A detailed description of the probe and feeder construction is given in Carrel,[3] pages 184 and 185.

In the second method of probing, the dipole currents were sampled by a shielded loop which was suspended directly over the feeder and moved up and down the antenna parallel to the feeder. The loop was oriented in such a way that the feeder was normal to a plane containing the loop. Thus the loop did not respond to the feeder current, but only to that component of each dipole current parallel to the dipole axis. This method gave more consistent and more easily analyzed results than the first method. Furthermore, agreement of the k-β diagram with the far-field patterns was better, and data were obtained from which it was possible to compute far-field patterns.

Although the magnetic field sampled by the probe at any one position is produced by several nearby dipoles, the principal contribution to the field close to any one dipole is due to that dipole itself. The readings that were of the greatest interest, therefore, were those taken when the probe was directly over each of the dipoles. Readings were taken at intermediate points for the sake of continuity; the smooth curves connecting all of these points are those given in Figures 15 and 16. But the principal emphasis in plotting the k-β diagram was given only to those points taken at the dipole locations.

Figure B.1 shows the phase measurement circuit. The Diagraph is connected to give readings of the phase angle of the dipole currents (sampled by the probe) relative to a reference signal (sampled from the oscillator output by one of the General Radio Type 874-GA cutoff attenuators). A polar-coordinate chart was used on the Diagraph*.

A detailed description of the measurement procedure is not given here; after the oscillator was adjusted to the desired frequency and the deflection of the light spot on the Diagraph peaked with the two pairs of tuning stubs, the Diagraph was operated in accordance with the instruction manual furnished with it. But two features of the circuit should be mentioned. First, since the Diagraph is reported to work better with a CW than a modulated signal, the modulation necessary

---

* Since the radial coordinate of the chart (Rohde and Schwarz type 35611/1658) is calibrated in decibels, amplitude readings were occasionally taken by this method also. Those presented in this report, however, were obtained by the method of Section B.3.

for observing the frequency meter output was imposed only on a small portion of the oscillator signal, obtained through the first of the two cutoff attenuators. The required components are shown in the "Frequency Measurement Section" of Figure B-1. Secondly, a new plexiglass screen was substituted for the original one on the Diagraph. On this new screen, the polar coordinate chart was fastened with one pin in the center, instead of two pins at the edge as in the original screen. This center pin featured a spring-loaded arrangement which caused the chart to turn normally with the screen, but allowed it to be rotated with respect to the screen whenever necessary. Since it was desired to establish the phase of the current in the first dipole as phase reference or "zero-phase", the Diagraph phase indicator was first peaked with the probe over the first dipole; then the chart rotated, while the screen was held fixed, until the zero-degree line of the chart fell over the light spot. By this means it was also possible to compensate for changes in the phase shift of the signal through the variable attenuator whenever the attenuator setting was changed. Such changes were often necessary to keep the light spot in view on the chart.

Figure B-2 is a photograph of the bench used for phase measurements (and also for amplitude and impedance measurements). The antenna mounted on the right-hand end of the bench is UPHDA-3. The loop probe is not shown; the probe connected to the equipment in this photograph is the voltage probe mentioned earlier in this section. When measurements were being taken, the bench was rolled up to an anechoic chamber so that the antenna extended into the chamber. The perforated aluminum screen shielded the equipment from stray radiation.

When the probe is moved along the antenna, the coaxial cable connected to it must bend. This flexing introduces some degree of change in phase shift through the cable, depending on the type of cable and how sharply it is bent. To keep this flexing (and its effect on measured data) to a miniumum, the excess cable is taken up on the large wheel, shown above the left-hand end of the bench. The signal is fed through a rotary joint in the hub of the wheel. A test showed that the phase shift of a signal through the cable when completely wound on the wheel was so close to the phase shift when the cable was unwound that the difference was almost unmeasurable.

One important feature of this apparatus, not shown in the photograph, must be mentioned. Whenever phase or amplitude measurements were being made, a portion of the antenna next to the screen and including the last three dipoles was enclosed in a large block of microwave absorber. The purpose of this material was to absorb the wave propagating along the antenna from the feed point, at those

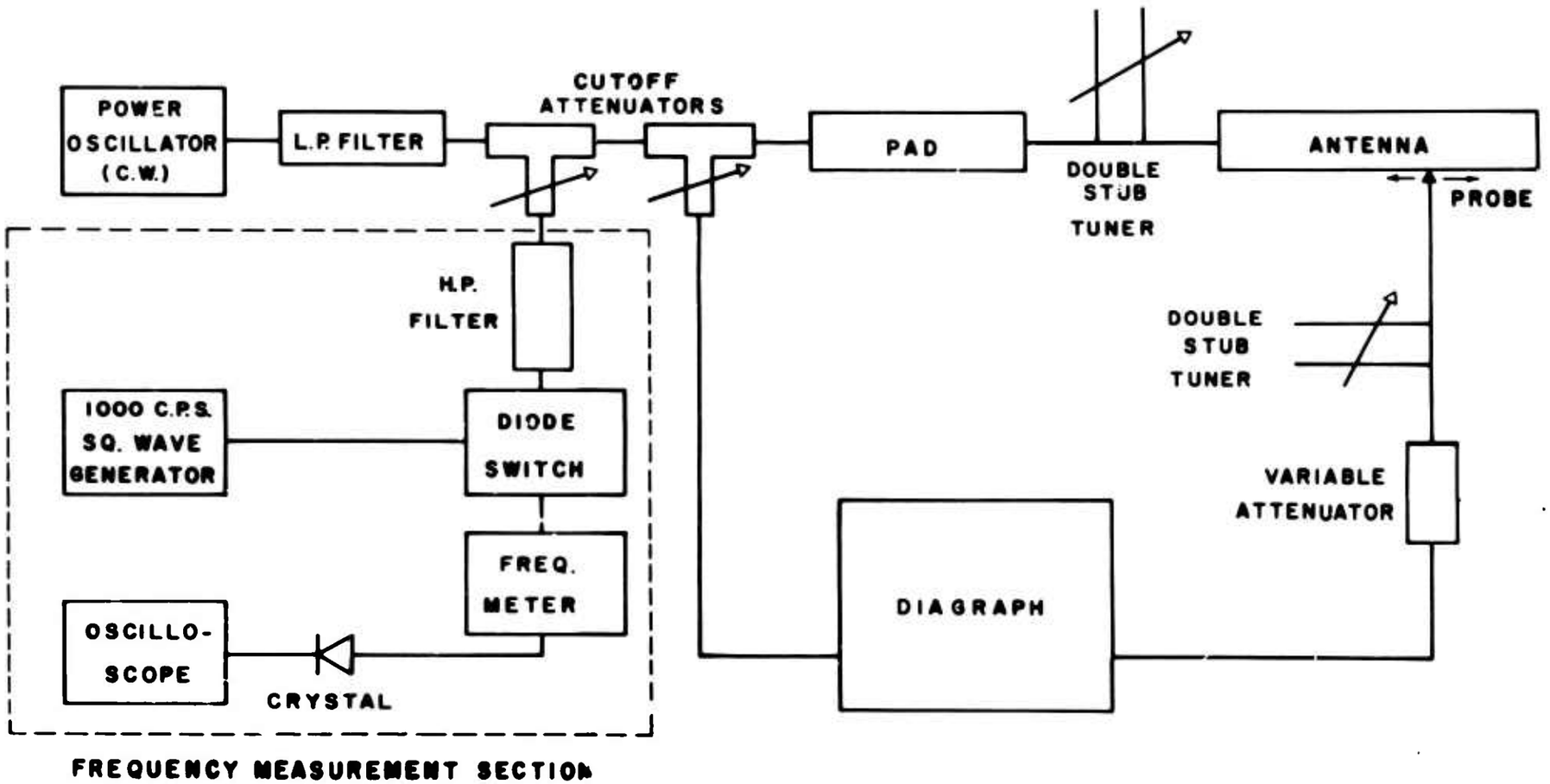

Figure B-1. Block diagram of phase-measurement apparatus

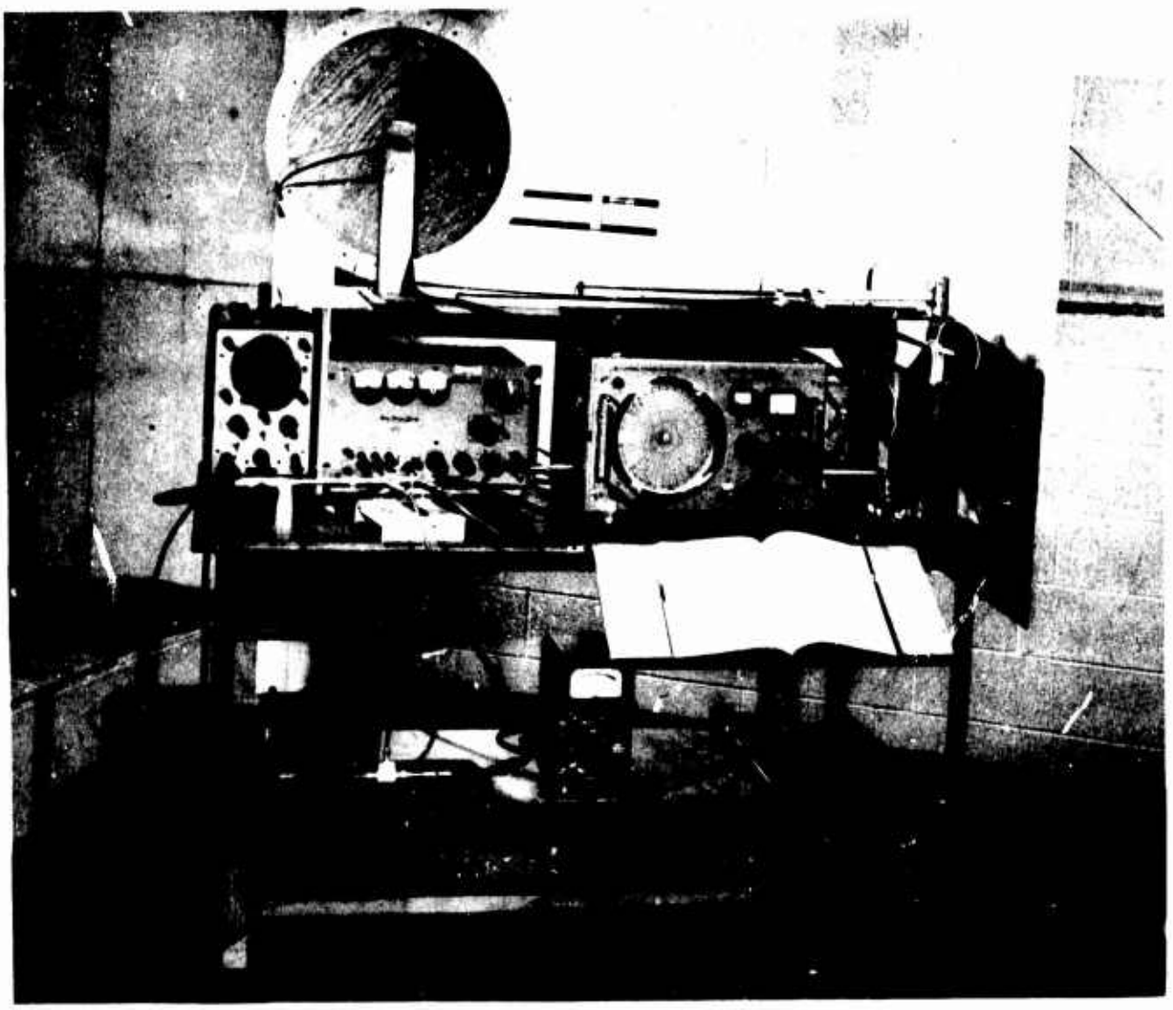

Figure B-2. Laboratory equipment connected for phase measurements

frequencies where attenuation per cell was low, and to keep the wave from being reflected back toward the feed point and interfering with the measurements of the incident wave.

B.3 Near-Field Amplitude Measurements

Figure B-3 shows the circuit used for measurements of the amplitude of the near field. The antenna and probes were mounted in exactly the same way as for phase measurements.

Two methods of recording amplitude data were provided. In one, a standing-wave amplifier gave a reading of the relative amplitude at each probe position; data were recorded point-by-point. As in the phase measurements, the reading obtained with the probe directly over the first dipole was used as the reference level; amplitudes at other points were read in decibels above or below this value. In the other method, a rectangular chart recorder was used to obtain a continuous plot of amplitude as a function of distance. The chart drive was controlled by a selsyn generator mounted on the probe carriage on top of the bench. A gear on the generator shaft was turned by a gear rack fixed on the bench. Even with this system, the standing-wave amplifier was used for initial tune-up procedures, and the signal was switched over to the recorder only for the actual plotting.

The amplitude plots in Figures 1.15 and 1.16 were traced directly from the recorder charts.

For these measurements, the RF oscillator was modulated directly by a 1000 cps square wave to satisfy the requirements of the SWR amplifier and the recorder.

B.4 Impedance Measurements

In Figure B-4 is shown the circuit that was used for impedance measurements on all LPHDA models. The "Frequency Measurement Section" is identical to that shown in Figure B-1. Since only a small signal is needed to drive the Diagraph, this signal was taken off through a cutoff attenuator and the bulk of the power oscillator output was dissipated in the "matched load", capable of handling several watts. In some measurements an oscillator with lower output power was used; in these cases the oscillator output was fed directly to the Diagraph through a variable attenuator.

Impedance measurements were performed according to instructions furnished with the Diagraph, with one modification. This modification was necessitated by the fact that the impedances desired were those referred to the antenna

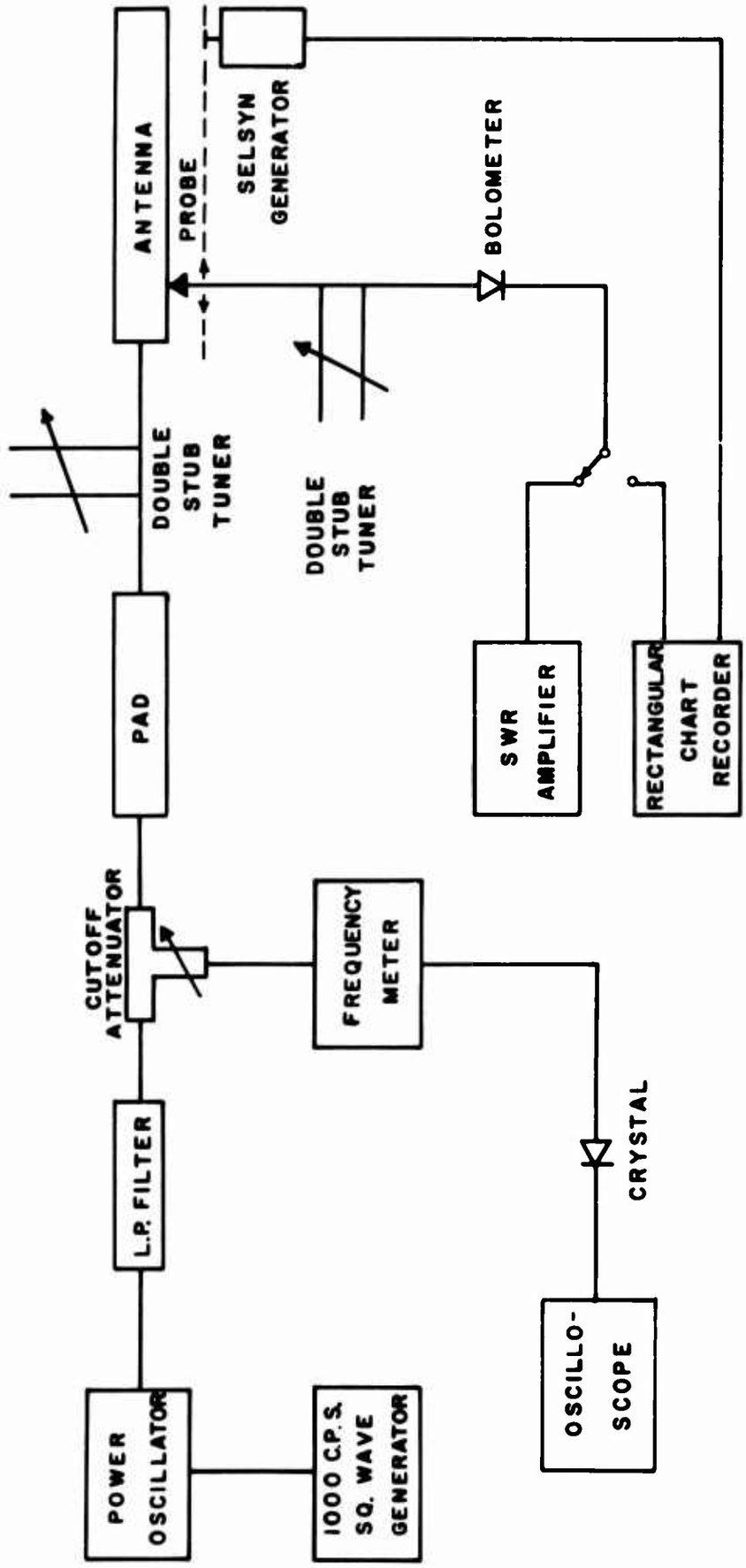

Figure B-3. Block diagram of amplitude-measurement apparatus

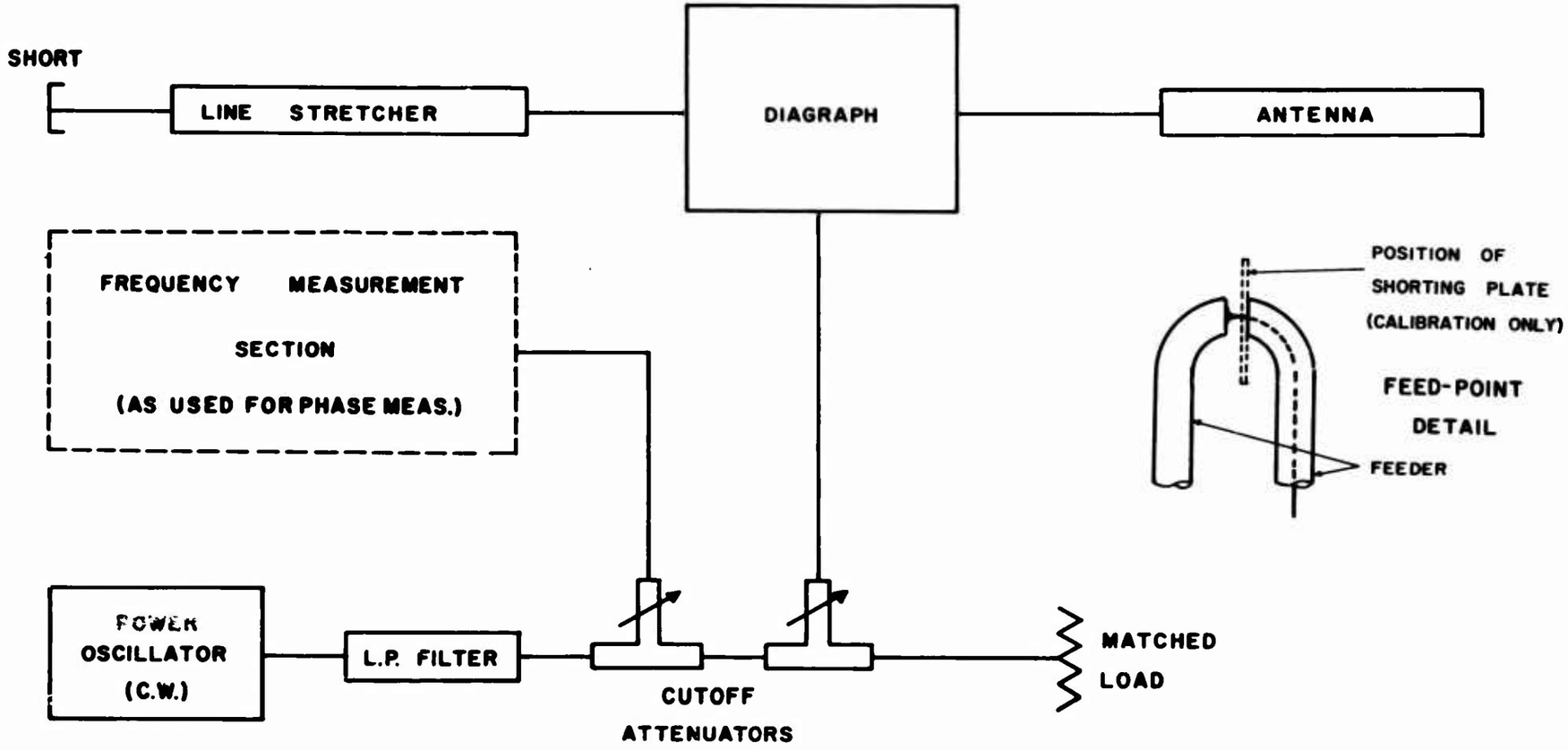

Figure B-4. Block diagram of impedance- measurement apparatus

feedpoint, not to the input cable connector. If a straight, uniform cable is used to connect a load to the Diagraph, impedance measurements may easily be referred to the end of this cable simply by connecting an identical cable to the reference line on the Diagraph, and short-circuiting this cable at its other end. In LPHDA measurements, however, the cable was small (RG-141), single-shielded, and bent sharply at the feedpoint. It was found that another cable could not be constructed for reference purposes that was the same electrical length as the antenna feed cable at all frequencies. Therefore, to the end of a piece of RG-141 cable leading from the reference input of the diagraph was connected a line stretcher, calibrated in millimeters and shorted at its other end. As a first step, this line stretcher had to be calibrated at all frequencies at which impedance measurements were desired so that its length plus the length of the piece of RG-141 cable connecting it to the Diagraph was electrically the same as the length of the antenna feed cable from the Diagraph to the feedpoint of the antenna. This was done by shorting the antenna cable at the feedpoint, as shown in the "Feed-Point Detail" in Figure B-4. At each frequency, using the Diagraph as an indicator, the line stretcher was adjusted to match up the electrical lengths of the two lines. Afterwards, the shorting plate was removed from the antenna feed-point and the impedance was measured in the conventional manner; for each frequency the line stretcher was reset to the proper value determined for that frequency in the calibration procedure.

Measurements of the resonant frequencies of individual helical monopoles were made by conventional impedance-measurement techniques, using a PRD standing-wave indicator. The frequency at which the impedance plot crossed the real impedance axis on the Smith Chart was the resonant frequency. All such measurements were made with the monopoles mounted above a 16 foot square ground screen. Resonant frequency measurements on helical dipoles were made on a Lecher-wire arangement which was probed by a small shielded loop. The procedure was similar to that used with a conventional slotted line.

B.5 Far-Field Pattern Measurements

Measurements of the far-field radiation patterns were made on the free-space pattern range installed on the roof of the old Antenna Laboratory. The antenna is mounted on a rotating mast; a polar chart recorder synchronized with the rotator is used to plot the field intensity as a function of position. A fixed antenna transmits a signal to the test antenna, whose output is connected through a

bolometer (or crystal, if the signal is weak) to an amplifier which drives the recorder pen in a radial direction over the chart. The resulting plots are proportional to field intensity; their radial coordinates must be squared to give the power pattern. Half-power beamwidths, therefore, are obtained by measuring the angle within which the measured field intensity is equal to or greater than 0.707 times the peak intensity.

UNCLASSIFIED

Security Classification

DOCUMENT CONTROL DATA - R & D

Security classification of title, body of abstract and indexing annotation must be entered when the overall report is classified)

1 ORIGINATING ACTIVITY (Corporate author) Antenna Laboratory, Department of Electrical Engineering, Engineering Experiment Station, University of Illinois, Urbana, Illinois	2a. REPORT SECURITY CLASSIFICATION UNCLASSIFIED 2b. GROUP

3 REPORT TITLE

BROADBAND ARRAYS OF HELICAL DIPOLES

4 DESCRIPTIVE NOTES (*Type of report and inclusive dates*)

Part 2 of Final Report, 1 June 1962-31 August 1963

5 AUTHOR(S) (*First name, middle initial, last name*)

D. T. Stephenson and P. E. Mayes

6 REPORT DATE January 1964	7a. TOTAL NO. OF PAGES 57	7b. NO OF REFS 11
8a. CONTRACT OR GRANT NO NEL 30508A b. PROJECT NO c. d.	9a. ORIGINATOR'S REPORT NUMBER(S) Technical Report 2 9b. OTHER REPORT NO(S) (*Any other numbers that may be assigned this report*)	

10 DISTRIBUTION STATEMENT

Distribution of this document is unlimited.

11 SUPPLEMENTARY NOTES	12 SPONSORING MILITARY ACTIVITY Navy Electronics Laboratory San Diego, California 92152

13 ABSTRACT

This report deals with the problem of reducing the resonant length of radiating elements of log-periodic dipole antenna arrays by the use of helical dipole elements. Some consideration is given also to the problem of boom length shortening. Reduced size log-periodic arrays are required to make practical shipborne applications in the high frequency band at frequencies as low as 8 MHz. Several reduced scale models were built using helical dipole elements and compared with similar designs using linear dipole elements. Directive gains and impedance characteristics were compared. An element shortening factor of 0.54 was used. Some mixed dipole arrays, where only the longer low frequency elements were shortened, also were tested.

Conclusions are that helical dipoles are useful and practical size-reduced elements for log-periodic arrays. However, boom length is increased by dipole length shortening and antenna performance somewhat impaired. The most practical design is a log-periodic mixed dipole array. Measurement techniques are treated in an appendix.

DD FORM 1 NOV 65 1473 (PAGE 1)

S/N 0101-807-6801

UNCLASSIFIED

Security Classification

14 KEY WORDS	LINK A		LINK B		LINK C	
	ROLE	WT	ROLE	WT	ROLE	WT
Antenna Arrays						
Helical Antennas						
Log Periodic Antennas						